University of Alberta

Study of the Rag Layer: Characterization of Solids

by

MadjlessiKupai, Morvarid (April)

A thesis submitted to the Faculty of Graduate Studies and Research in partial fulfillment
of the requirements for the degree of

Master of Science
in
Chemical Engineering

Chemical and Materials Engineering

©Morvarid Madjlessikupai
Fall 2012

Edmonton, Alberta

ABSTRACT

During separation of emulsified water from oil, a viscous intermediate layer builds up between water and oil phases. This layer which is referred to as rag layer disrupts emulsion destabilization and water removal. The present research is intended to better understand the formation of a rag layer and its properties, so that rag layer formation can be prevented.

Two industrial froth samples are considered: one readily forms a rag layer and the other does not. Characterization of emulsion and contained solids is completed to elucidate the key properties that result in rag layer formation. Key differences between the solids that formed and did not form rag layer were identified as: (i) organic contaminates of rag-forming-solids contain more aromatic compounds as compared with those of the non-rag-forming solids; and (ii) rag-forming solids are more hydrophobic. Moreover, mineralogy analysis of these two solids showed that rag-forming-solids contain a considerable amount of iron-based minerals, such as siderite and pyrite. Such research has provides a better understanding of these complicated, troublesome systems.

ACKNOWLEDGMENT

TABLE OF CONTENTS

TABLE OF FIGURES

LIST OF NOMENCLATURES

Latin symbols

G Gibbs free energy (j)

$\Delta_{int}G$ Detachment energy, energy to remove particles from oil-water interface (j)

f_i Frequency, mass fraction

r Particle diameter (m)

t Time (s)

Greek symbols

γ_{ow} Surface tension at oil-water interface (N/m)

γ_c Critical surface tension (mN/m)

θ_{ow} Contact angle at oil-water interface

Acronym symbols

CNRL   Canadian natural resources limited

DSA   Drop shape analyzer

FTIR   Fourier transform infrared spectroscopy

PC   Primary cyclone

PSC   Primary separation cell

PSV   Primary separation vessel

RPM   Rotation per minute

SAGD   Steam assisted gravity drainage

SC   Secondary cyclone

TGA   Thermal gravimetric analysis

XRD   X-ray diffraction

1. INTRODUCTION

1.1. OIL SANDS

The unconsolidated sand deposits found in northern Alberta such as, Athabasca, Peace River and Cold Lake, contain oil of a very high viscosity and molecular mass. Such deposits are commonly referred to as 'oil sands' with the viscous oil known as bitumen. These oil sands typically contain 80-85wt.% mineral solids, 6-14 wt.% bitumen and the remaining few percent is water.

Bitumen production is either achieved through surface mining of the oil sands ore followed by extraction, or in-situ processing such as Steam Assisted Gravity Drainage (SAGD), or cyclic steam simulations (CSS), (Samiei 2007; Bott 2005).

The processability of the oil sands ore is often dependent upon the 'grade' which is defined by the bitumen and fine solids content. It is often observed that good ores (high bitumen, low fines content) process better than poor ores (low bitumen, high fines content) (Liu et al. 2004; Zhou et al. 1999; Masliyah et al. 2008). In addition to the solids concentration, the physical and chemical properties of the solids, such as particle size, mineralogy, hydrophobicity and zeta potential impact the processing performance of an ore, (Liu et al. 2005; Liu et al. 2004; Liu et al. 2004; Zhou et al. 1999).

1.2. SEPARATION PROCESS

The water-based extraction process is widely used to recover bitumen from surface-mined oil sands ores. The mined ore is crushed and slurried with water in either; mixing boxes, stirred tanks, cyclo-feeders (Syncrude) or rotary breakers (Suncor and Shell Albian). The slurry is then transferred to the extraction plant via hydrotransport pipelines or tumblers. During transportation fluid shear breaks up coarse lumps of sand and enhances bitumen liberation from the sand grains. Chemical additives such as sodium hydroxide are often added to the slurry to optimize the effective interaction potential between bitumen, solids and air. Bitumen droplets attach to air bubbles in the hydrotransport pipeline, lowering the apparent density of bitumen and hence, enabling successful separation through flotation. Flotation takes place in a gravity separation

vessel, known as either; the primary separation vessel (PSV), separation cell (Sep Cell) or primary separation cell (PSC).

Recovered froth from separation typically consists of 60% bitumen, 30% water and 10% solids by mass. Further treatment of the froth is required to produce bitumen with minimal water and solids. To 'clean' the recovered bitumen, froth is de-aerated and diluted (mixed) by solvent addition to increase the density difference between water and bitumen, and to reduce bitumen viscosity. Inclined plate settlers, cyclones and/or centrifuges are used to separate the unwanted components from bitumen. The type of solvent used to dilute bitumen froth is somewhat company specific with Suncor, CNRL and Syncrude operations using naphtha, and Shell Albian using a paraffinic diluent, mainly C_5-C_6 mixture.

Paraffinic (C_5-C_6) and aromatic (naphtha) diluents behave differently. With paraffinic diluents, asphaltene precipitate forming aggregates that trap water and solids in the diluted froth. This enhances separation and eliminates the need for cyclones and centrifuges, but reduces bitumen recovery since half of the asphaltenes, 8-10% of the total bitumen, are precipitated and removed from the product stream. Typically, bitumen recovery using such practice is about 88–95%. However, in naphthenic froth treatment, solvent is used at a dilution ratio in which asphaltene does not precipitate, hence, enhanced gravity separation is necessary, (Samiei 2007; Masliyah et al. 2008; Masliyah 2009).

1.3. DEFINING THE RAG LAYER PROBLEM

As previously discussed, unwanted material, water and solids, must be removed from froth prior to upgrading in order to maintain downstream specifications. This is achieved by increasing the density difference between bitumen and water to assist separation. Gravity separation of the lighter diluted organic phase may be enhanced through the use of hydrocyclones or centrifuges.

During separation a viscous layer sometimes forms at the planar interface between the oil and water phases. The viscous layer is referred to as the 'rag layer' which consists of oil, water and solids, (Czarnecki et al. 2007).

In the water-based extraction process, rag layers are known to form during froth treatment. Rag layer formation on the inclined plate settler (IPS) can become problematic since the rag layer thickness increases with time; eventually overflowing to contaminate the oil stream (product), leading to fouling of upgrading equipment, (Saadatmand and Yarranton 2008). Rag layers can also form in the refinery both at the early stages of processing (desalting) and the final stages (collection of slop oil), (Ohsol 1999).
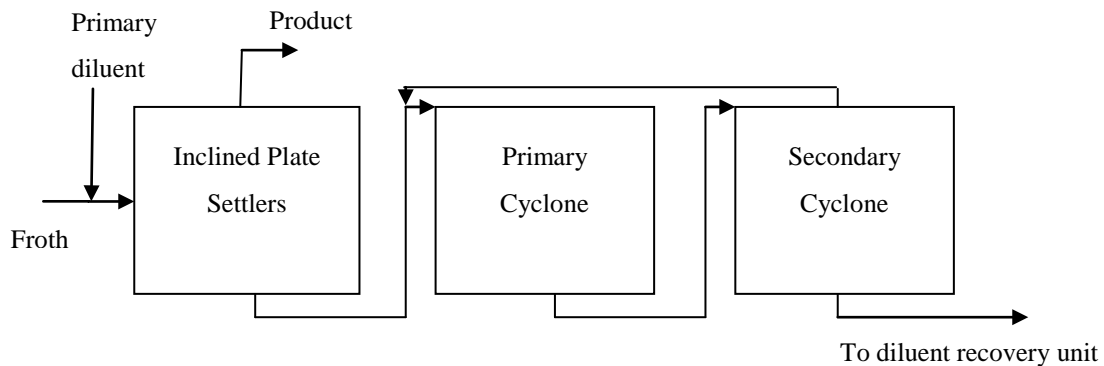
Figure 1-1: Diagram of naphthenic froth treatment process. Redrawn from (Masliyah 2009)

The formation of a rag layer will hinder the dewatering capabilities of processing equipment, (Czarnecki et al. 2007). Settling water droplets and solids can become trapped within the rag layer, along with diluted bitumen that is not recoverable, leading to a reduction in bitumen recovery and potential contamination of the product stream.

The mechanism by which rag layers form and the gradual 'trapping' of water, solids and diluted bitumen is debated in the literature without a clear understanding.

Varadaraj and Brons (2007) suggest that the rag layer is a micro-heterogeneous complex fluid of oil-in-water-in-oil, multiple emulsions coexisting with oil-in-oil, solids-in-oil and water-in-oil dispersions throughout a continuous oil phase. Figure 1-2 illustrates their observation. The dispersed dark oil is a phase separated, incompatible oil fraction with a possible higher molecular weight that disperses as the sample is heated to 75°C. The authors refer to the rag layer as a complex fluid.

Czarnecki et al. (2007) described the rag layer as a mixture of flocculated water droplets, fine solids and multiple emulsions. An image of the rag layer coming from naphtha

diluted bitumen is shown in Figure 1-3, in which multiple emulsions of oil-in-water-in-oil can be observed.

Saadatmand and Yarranton (2008) observed emulsified water droplets and solid particles dispersed in a continuous phase of n-heptane diluted bitumen at D/B ratio of 0.66 g/g, with no formation of a complex emulsion, see Figure 1-4. The authors suggest that the rag layer is a loose structure of layered materials at the interface, rather than a consolidated matrix of solids and emulsions.

Gu et al. (2007) believe that the rag layer is a complex dispersion with a structure described as silt sludge with entrained oils. Unlike the studies which observed emulsified water droplets, spherical water droplets could not be identified in the rag layer even after excessive dilution with naphtha and toluene. An image of the rag layer observed by Gu et al. (2007) is illustrated in Figure 1- 5.

It is universally accepted that the rag layer consists of oil, water and solids, with the layer preventing complete separation of the two fluid phases, reducing the overall recovery of oil. Such problems have invigorated research into better understanding the formation of a rag layer, leading to a greater knowledge of rag layer prevention and possible methods to 'break' its formation.
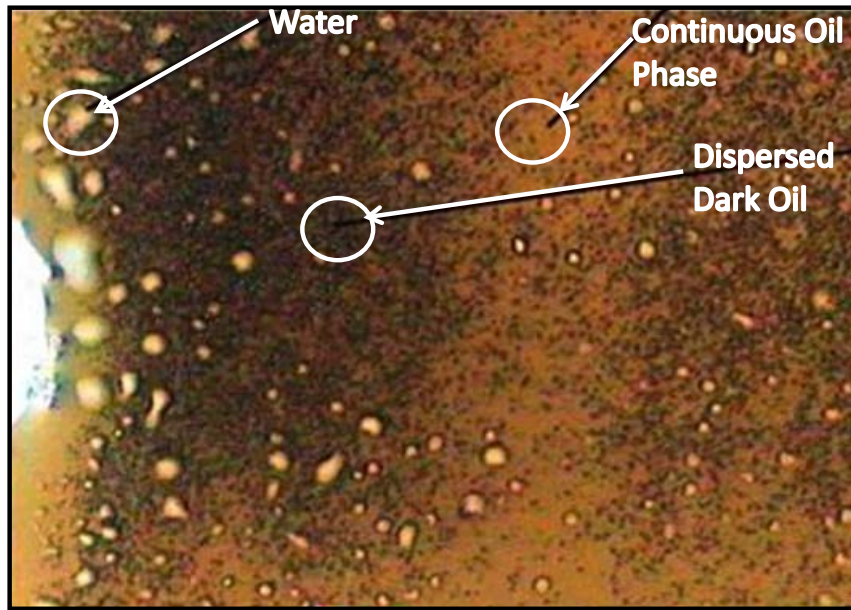
Figure 1-2: Microscope image of a rag layer recovered from a well head emulsion. Water (lighter) and oil droplets (darker) are dispersed in a continuous oil phase, (Varadaraj and Brons 2007).

4
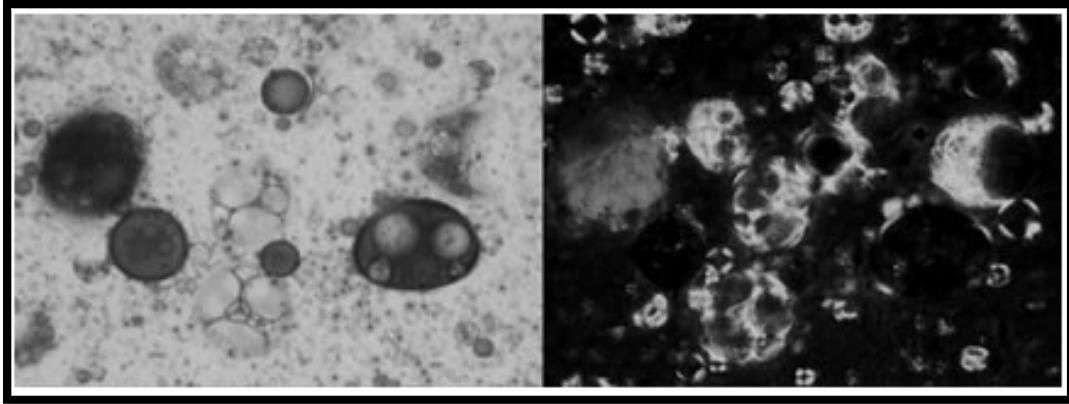
Figure 1-3: Microscope image of a multiple emulsion (o/w/o) in water-diluted bitumen, (Czarnecki et al. 2007). Left: normal illumination, Right: cross polarized light.
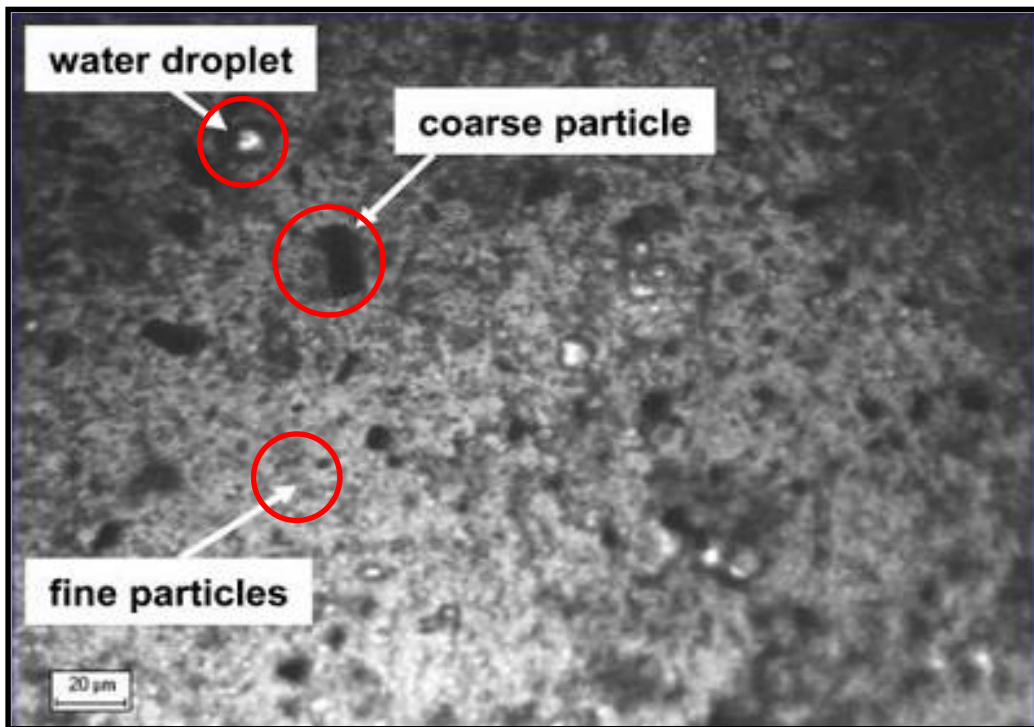
Figure 1-4: Microscope image of a rag layer sample obtained by centrifuging a froth sample recovered using a Denver flotation cell, (Saadatmand and Yarranton 2008).
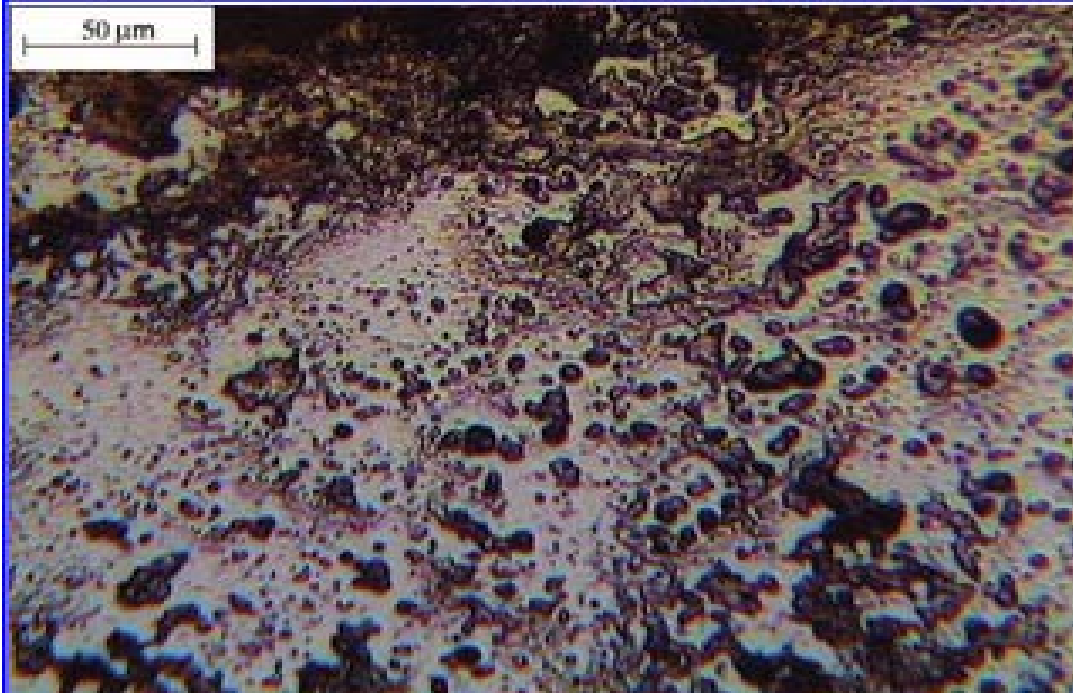
Figure 1-5: Microscope image of a rag layer after excessive dilution with naphtha. Spherical water droplets are not clearly observed, (Gu et al. 2007).

1.4. SUGGESTED MECHANISMS FOR THE FORMATION OF A RAG LAYER

Three mechanisms are used to describe rag layer formation:

Mechanical barrier: accumulation of oil-wet material at the planar oil-water interface creates a barrier that prevents dispersed water droplets and solids from crossing the interface and entering the water phase.

Intermediate density: the rag layer density (composed of water, oil and solids) favors stability between the two fluid phases.

Slow coalescence: rag layer accumulation and the build-up of interfacial material hinder droplet coalescence, such that settling droplets become trapped in the stable network.

1.4.1.   MECHANICAL BARRIER

Saadatmand and Yarranton (2008) studied the mechanical barrier theory. Precipitated asphaltenes were dispersed in n-heptane at a concentration of 10 g/L. The dispersion was gently deposited onto a water-oil interface, with co-precipitated solids (0.34 wt.% fines).

Large water droplets (1 mm) were then deposited through the n-heptane phase coming to rest at the oil-water interface. The authors commented that the droplet-homophase coalescence became inhibited by the increased accumulation of asphaltenes and fine solids at the interface.

Repeat experiments using Heptol 50/50 (heptane: toluene), in which asphaltenes are soluble, prevented the formation of an interfacial barrier hence, water droplets were observed to coalesce upon contact with the water subphase.

Such experiments confirmed that a mechanical barrier which impedes coalescence leads to rag layer formation. However, to validate the hypothesis, continual disruption of the rag layer should prevent its formation.

Saadatmand and Yarranton (2008) further studied the mechanical barrier theory by preparing two samples from heptane diluted froth with precipitated asphaltenes. The authors used a stepwise centrifugation technique (discussed in Section 1.6) to create the rag layer. The two samples were treated differently, one sample stirred after each centrifuge step to break the rag layer. Even with continual disruption of the rag layer, there was no difference between the two rag layer volumes after several centrifugation steps. This observation would suggest that the mechanical barrier is not the major contributor to rag layer formation.

1.4.2.   INTERMEDIATE DENSITY

Czarnecki et al. (2007) proposed that the rag layer is a mixture of flocculated water droplets and fine solids, see Figure 1-3. The authors suggest that multiple emulsions of oil-in-water-in-oil (continuous phase) produce droplets with an apparent density in-between the water and organic phase densities. As a result, accumulating water droplets were prevented from coalescence due to their low inertial contribution and the build-up of interfacial material.

1.4.3.   SLOW COALESCENCE

In order to separate an emulsion (fine droplets) two physical phenomena must occur:

- Droplet coalescence: the merging of two droplets to form one larger droplet, and the merging of a droplet with its homophase.
- Droplet sedimentation: settling through a continuous oil phase; governed by the fluid densities, droplet diameter, oil phase viscosity and force (gravity) (Frising et al. 2006).

As a first order approximation, the separation rate can be reasonably described by Stokes' equation. However, such an equation does not account for the coalescence efficiency of droplets, nor the hindered settling contribution. To achieve a high rate of separation there should be minimal resistance to droplet-droplet and droplet-homophase coalescence events. The rate of separation can be impeded by the accumulation of surface-active species such as; fine solids and asphaltenes. A reduction in the coalescence rate may eventually lead to the build-up of a rag layer as droplets continue to settle and accumulate at the oil-water interface, (Binks and Lumsdon 2000b; Freer and Radke 2004; Arditty et al. 2003; Whitesides and Ross 1995; Saadatmand and Yarranton 2008).

1.5.   EMULSION STABILIZERS

Interfacially active species such as; asphaltenes, resins, natural surfactants and fine solids have been shown by many researchers to improve interfacial rigidity and hence contribute to the overall stability of an emulsion, (Ali and Alqam 2000; Sztukowski and Yarranton 2005; McLean and Kilpatrick 1997; Kotlyar et al. 1998; Kotlyar et al. 1999; Yan et al. 2001; Kilpatrick et al. 1997).

In oil sands recovery, asphaltenes and fine solids are widely recognized as the main components in stabilizing emulsions (water-in-bitumen), (Kilpatrick et al. 1997). These two components have the ability to stabilize water-in-diluted-bitumen emulsions in the absence of the other. The stabilizing capacity of a water-in-diluted bitumen emulsion is considerably reduced when they are removed from the system, (Yan et al. 1999).

1.5.1. ASPHALTENES

Bitumen is a complex mixture of many different chemical species, of which asphaltenes are often considered the most problematic during processing, (Strausz et al. 1992). Asphaltenes are described by their solubility classification; insoluble in light alkanes such as pentane, hexane or heptane and soluble in aromatic solvents such as benzene and toluene. They are known to have polycyclic aromatic clusters, substituted with different alkyl side chains [polyaromatic core – several aromatic rings and aliphatic side chains], with an approximate molecular weight in the range 500-1500 Dalton. Asphaltenes contain the highest amount of heteroatoms (O, S, N) and transition metals (Ni, V) among all other bitumen constituents, (Sjoblom et al. 2003).

The condensed aromatic sheets are interconnected by sulfide, ether, aliphatic chains, or naphthenic ring linkages and heterocyclic atoms (O, N, S). The transition metals (vanadium, nickel) mainly exist in the form of porphyrin by chelate or coordinate bonds (Yen et al. 1969; Mullins, and Sheu, 1998). It has been revealed that the oxygen-containing groups of asphaltenes are mainly carbonyl, carboxylic and hydroxylic, (Kilpatrick and Spiecker 2001; Sjoblom et al. 2001b).

Different asphaltenes have different aromaticity, polarity and molecular size, which have been shown to affect the stability of an emulsion, (Mohamed et al. 1999;Yang et al. 2004). Asphaltenes are studied to better understand their structure and chemistry, and self-aggregation and interfacial activity at water/oil and solid/oil interfaces, (Wang 2011)

The aromatic sheets are able to associate through $\pi - \pi$ stacking, hydrogen bonding and acid-base interactions to form extended aggregates. These aggregates have a tendency to adsorb a sheath of aromatic resins. The aggregate size depends on: i) the aromaticity of a solvent, ii) temperature and iii) concentration of flocculants such as resins in solution, (Wang 2011). At high resin to asphaltene ratios, higher than 0.33 in some case studies (McLean and Kilpatrick 1997), asphaltene aggregates are less surface active since the resins are present to solvate the asphaltenes and their contribution to emulsion stability is reduced. At low resin to asphaltene ratios, the asphaltene aggregates remain surface active and adsorb at the water/oil interface, (McLean and Kilpatrick . 1997; Kilpatrick et al. 1997). See Figure 1-6.

The presence of aliphatic hydrocarbon chains and polar functional groups give asphaltenes a bi-wettability and hence, their interfacial activity, (Sjoblom et al. 2001a). Asphaltene aggregates adsorb at the water/oil interface forming a viscoelastic network. These asphaltene films act as a barrier to droplet coalescence, thus emulsion stability is observed to increase. The interfacial barrier is often described as a "skin" or "plastic film", (Kilpatrick and Spiecker 2001). See Figure 1-7.

With approximately 17% (by mass) of bitumen in the form of asphaltenes, the interaction of bitumen with water can result in the formation of an extremely stable emulsion, (Gu et al. 2006). However, Gu et al. (2006) found that only a fraction of these asphaltenes contribute to the formation of an interfacial film. Compared with the bulk, interfacial asphaltenes are characterized by a lower H/C ratio (higher aromaticity) and a higher O/C ratio (higher polarity).
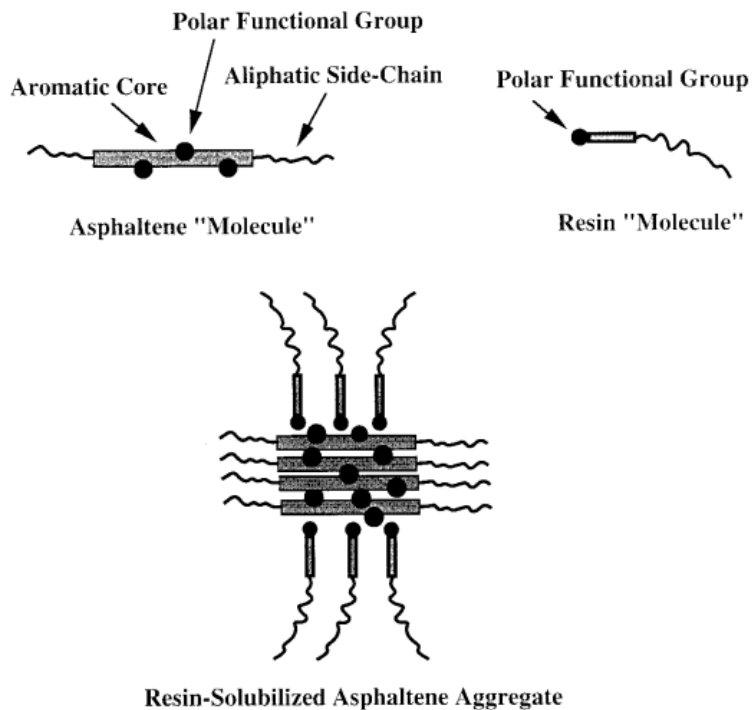
Figure 1-6: Interaction mechanism of asphaltenes and resins (Kilpatrick et al. 1997)

In order to disrupt and destabilize an asphaltene interfacial film, demulsifiers are added to change the film properties such as, composition, thickness and rigidity. Demulsifiers act either by interacting with the interfacial material and/ or by species replacement. Many researchers have shown a reduction in emulsion stability after the addition of a suitable

demulsifier, (Feng et al. 2009; Sjoblom et al. 2001b; Urdahl et al. 1993; Zhang et al. 2003; Binks and Kirkland 2002; Tambe and Sharma 1993).
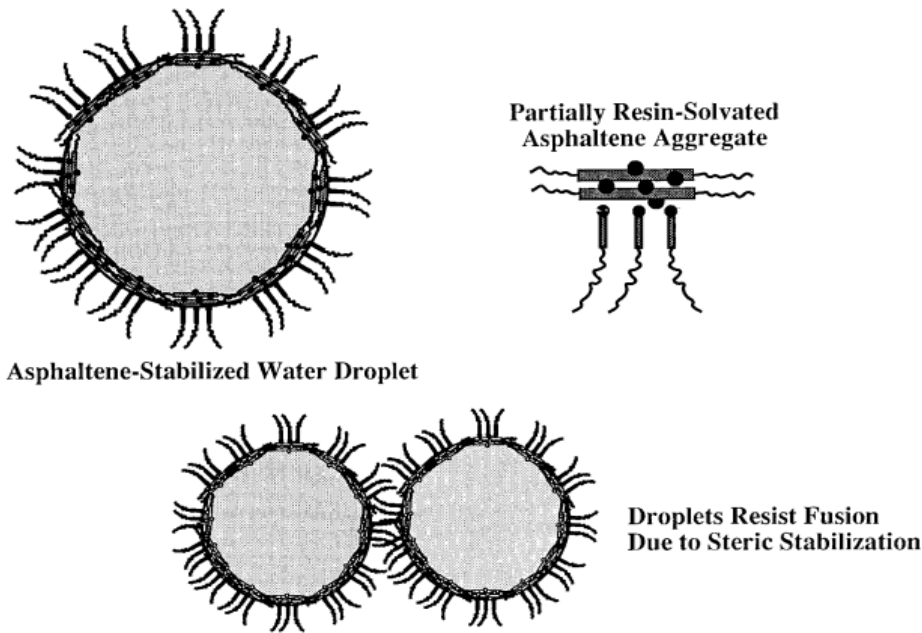
Figure 1-7: Adsorption of asphaltene aggregates at the water-oil interface (McLean and Kilpatrick 1997).

1.5.2. FINE SOLIDS

Fine solid particles have been shown by many researchers to stabilize both water-in-oil and oil-in-water emulsions, (Sztukowski and Yarranton 2005; Kotlyar et al. 1999; Yan et al. 2001; Bensebaa et al. 2000; Binks and Lumsdon 2000a; Angle et al. 2007). Figure 1-8 clearly demonstrates the impact of solids on improving emulsion stability (figure generated empirically). Two toluene-diluted-bitumen samples (with and without solids) were mixed with water. After a certain amount of time, the separated emulsion phases were measured. Clearly, the emulsion prepared with solids is more stable (no free water resolved) than the emulsion prepared in the absence of solids; more than half of the original water was resolved on a basis of 2:1 water-oil ratio, (Gu et al. 2002).
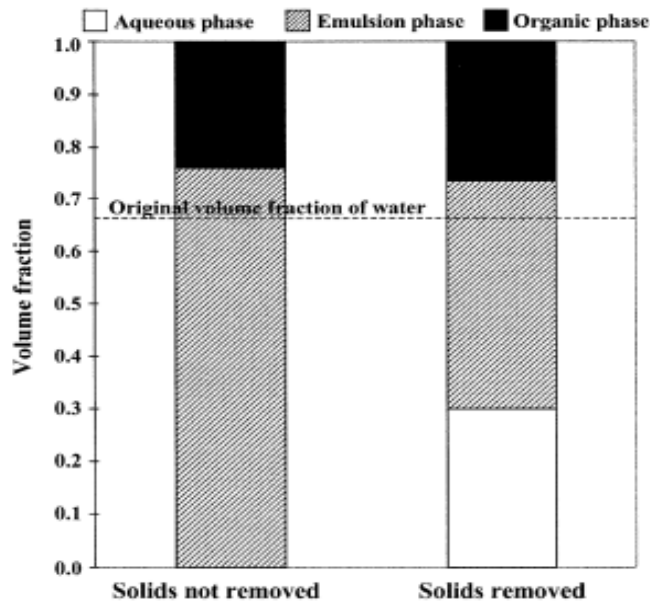
Figure 1-8: Stability of two water-in-diluted bitumen emulsions in the presence and absence of fine solids. Free water was resolved in the absence of solids, (Gu et al. 2002).

Further studies by Jiang et al. (2007) have shown that the presence of solids can have a detrimental effect on demulsifier performance. While complete separation of an asphaltene stabilized emulsion is observed, use of the same demulsifier[1] with particles and asphaltenes positioned at an interface has been shown to result in only partial separation. A study by Angle et al. (2007) reported similar observations on demulsifier performance after solid particles are added to the emulsion. The study showed that the surface properties of the solids were modified by the demulsifiers, altering their wettability (increasing hydrophobicity) and increasing their partitioning at the water-oil interface. Once at the interface, fine solids are able to hinder droplet coalescence through increased film rigidity and electrical double layer forces acting between approaching particles, (Yan et al. 2001; Tambe and Sharma 1993). If two droplets collide, coalescence may still be prevented by the mechanical rigidity and viscosity of the interfacial film, (Binks and Kirkland 2002). Depending upon the solids concentration and the particle-particle interaction strength, three-dimensional networks can form at the interface, possibly forming a 'bridge' between neighboring droplets, limiting droplet mobility and the potential for coalescence, (Sztukowski and Yarranton 2005; Binks and Kirkland 2002; Binks and Lumsdon 2000a).

---

[1] polyoxyethylene (EO)/polyoxypropylene (PO) alkylphenol formaldehyde resin

The ability of a particle to partition and stabilize an oil-water interface depends upon many factors such as, particle size, shape, surface area, density and wettability. It has been shown that solids larger than 8 μm do not modify the stability of a water-in-diluted-bitumen emulsion, (Yan et al. 1999). However, colloidal (few microns) and nanoparticles have been shown to significantly enhance the stability of emulsions, (Aveyard et al. 2003;Yan et al. 2001; Tambe and Sharma 1993; Gu et al. 2002).

The importance of wettability and its relation to emulsion stability has been considered by many researchers. Similar to a HLB scale, the effectiveness of a particle to position at an interface is described by its hydrophilic, hydrophobic nature. Hydrophilic particles (contact angle of less than 90°) are capable of stabilizing oil-in-water emulsions, while hydrophobic particles (contact angle greater than 90°) stabilize water-in-oil emulsions. Experiments have shown that the most stable emulsion is obtained when the contact angle approaches 90°, (Yan et al. 2001; Tambe and Sharma 1993). These observations are suitably described by the detachment energy equation (1-1) which shows a maximum when θ = 90°. The energy required to remove a spherical particle from an interface depends upon the contact angle, the contact area and the interfacial tension, (Aveyard et al. 2003; Binks and Lumsdon 2000b).

$$-\Delta_{int}G = \pi r^2 \gamma_{ow}(1 \pm \cos\theta_{ow})^2 \quad (1\text{-}1)$$

The solids associated with oil-field emulsions have been identified as aluminosilicate clays bearing heavy metals, with a typical particle size in the range of 100-200 nm diameters, (Kotlyar et al. 1998; Kotlyar et al. 1999; Bensebaa et al. 2000). Since these solids are exposed to aromatic polar organic components from the oil sands deposits, their surfaces become coated by asphaltenic material. Such interaction results in a bi-wettable solid.

Figure 1-9 is a schematic showing the coverage of organic matter and bitumen on a solid surface. The surface of the particles is not fully coated with organic matter with the clay surface partially exposed. The organic matters have characteristics of both asphaltenic and humic material. It is possible that the solids were exposed to plant humic matter prior to exposure to bitumen. The humic acids strongly interact with other polar molecules such as multi-ring components like asphaltenes. The bitumen components can potentially

adsorb onto exposed clays surfaces, humic-coated surfaces or overlap each other (Bensebaa et al. 2000).

Figure 1-10 illustrates how solid particles could contribute to emulsion stability, as the bi-wettable solids position at the interface of bitumen and water. Organic matter on the solids surface attracts heavy organic components and asphaltenic material, bridging the particles to form of a rigid film that prevents coalescence of droplets and increases emulsion stability, (Bensebaa et al. 2000; Kotlyar et al. 1999; Adegoroye et al. 2010).

The association of organic matter and mineral particles could be a loose or a tight binding complex. Different mechanisms are possible for these interactions, such as: electrostatic, van der Waals forces and hydrogen bonds.
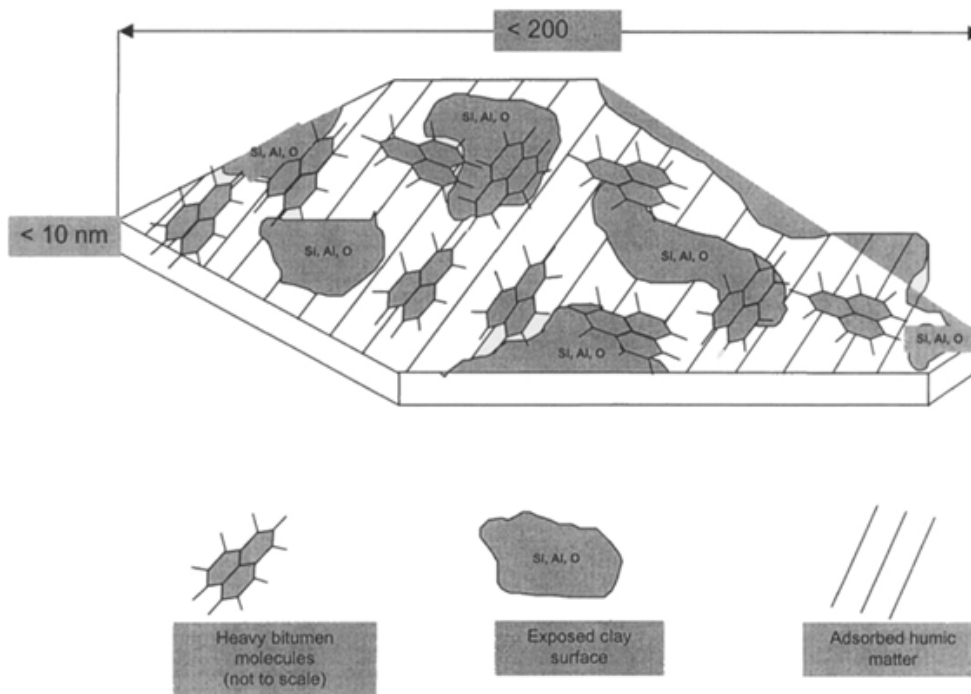
Figure 1-9: Simplified diagram of an organic coated clay particle, (Bensebaa et al. 2000).
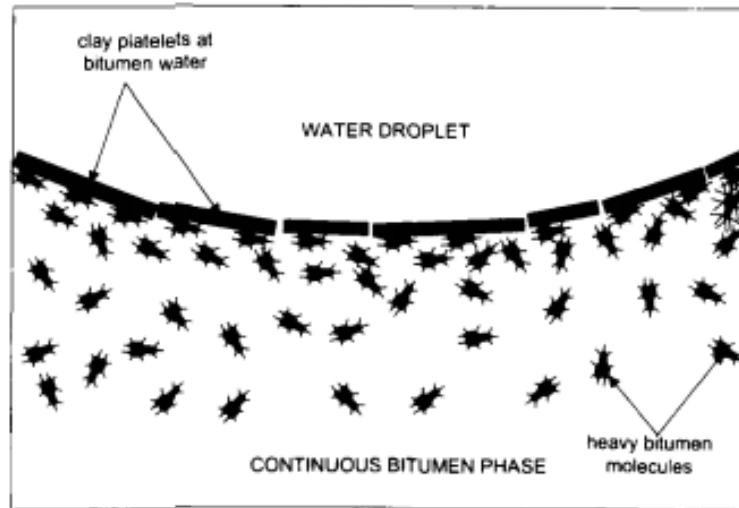
Figure 1-10: Stabilization of emulsion by clays and asphaltenes at the interface, (Bensebaa et al. 2000).

One of the mechanisms suggested for the adsorption of organic matter on solids is ligand exchange and anion exchange with hydrous oxides of iron and aluminum. Hydrous oxides present on the clay surface dominate surface reactions and encourage a cementation effect that leads to the strong aggregation and concretion and formation of a crust, (Adegoroye et al. 2010; Stevenson 1982; Tan 2009).

As discussed, solids contribute significantly to the stabilization of water-in-oil emulsions; as such their importance cannot be ignored when studying the mechanisms for rag layer formation and break-down.

1.6. RAG LAYER REPRODUCTION TECHNIQUES IN THE LABORATORY

It is often very difficult to maintain rag layer structure during in-situ sampling. Techniques and protocols are required to reconstruct the rag layer prior to laboratory testing. In an industrial separation vessel, the rag layer builds up gradually overtime, breaking as the weight exceeds the buoyancy contribution. To form a rag layer in a laboratory via continuous processing is often very difficult to achieve since the passage through pumps tends to break-down rather than form a rag layer, (Gu et al. 2007).

Czarnecki et al. (2007) proposed the following protocol to form a rag layer; i) prepare a 2 litre emulsion of water-in-naphtha-diluted-bitumen (N/B ~ 0.7), ii) centrifuge the stock emulsion to concentrate the interfacial material, and iii) remove the water and oil phases leaving the interfacial material in the centrifuge tube. More stock solution is then added and the process is repeated. Eventually enough interfacial material remains to be considered a rag layer.

Saadatmand and Yarranton (2008) developed a stepwise centrifugation method in which the recovered froth from a Denver flotation experiment was centrifuged at 500 rpm (26 g) for 5 minutes. After centrifuging four phases were observed: sediment bed, clear water, interfacial zone and clear oil. The volumes of each phase were recorded prior to a further 5 minutes of centrifugation at a higher rpm; increase of 500 rpm (in other words, the sample was initially centrifuged at 500 rpm and centrifuged a second time at 1000 rpm). This stepwise increase in centrifugation speed was continued until 4000 rpm (1600 g). At speeds higher than 2500 rpm the volume of the interfacial zone remained stable and was considered to be the sample rag layer.

Gu et al. (2007) developed an experimental setup to produce rag layers from diluted froth or diluted bitumen using a laboratory continuous process. The setup includes a 4 litre temperature controlled vessel which is filled with municipal water, see Figure 1-11. Froth or bitumen samples are diluted by naphtha addition prior to experiments at different naphtha to bitumen dilution ratios. The diluted froth or bitumen samples are introduced dropwise (1 – 5 mm droplets) from the base of the vessel, with droplet introduction ongoing during a two hour "wash cycle".

As the droplets cream through the aqueous phase, emulsified water and solids separate from the rising droplets, accumulating at the vessel base where they are regularly removed. The separated organic phase forms a layer on top of the aqueous sub-phase see Figure 1-11. Samples are taken from the organic phase through the sampling point indicated in Figure 1-11. After the first cycle, which runs for two hours, the organic phase is recycled into the vessel for another 6 cycles (12 hours). After continual recycling, a rag layer begins to form between the water and organic phases.
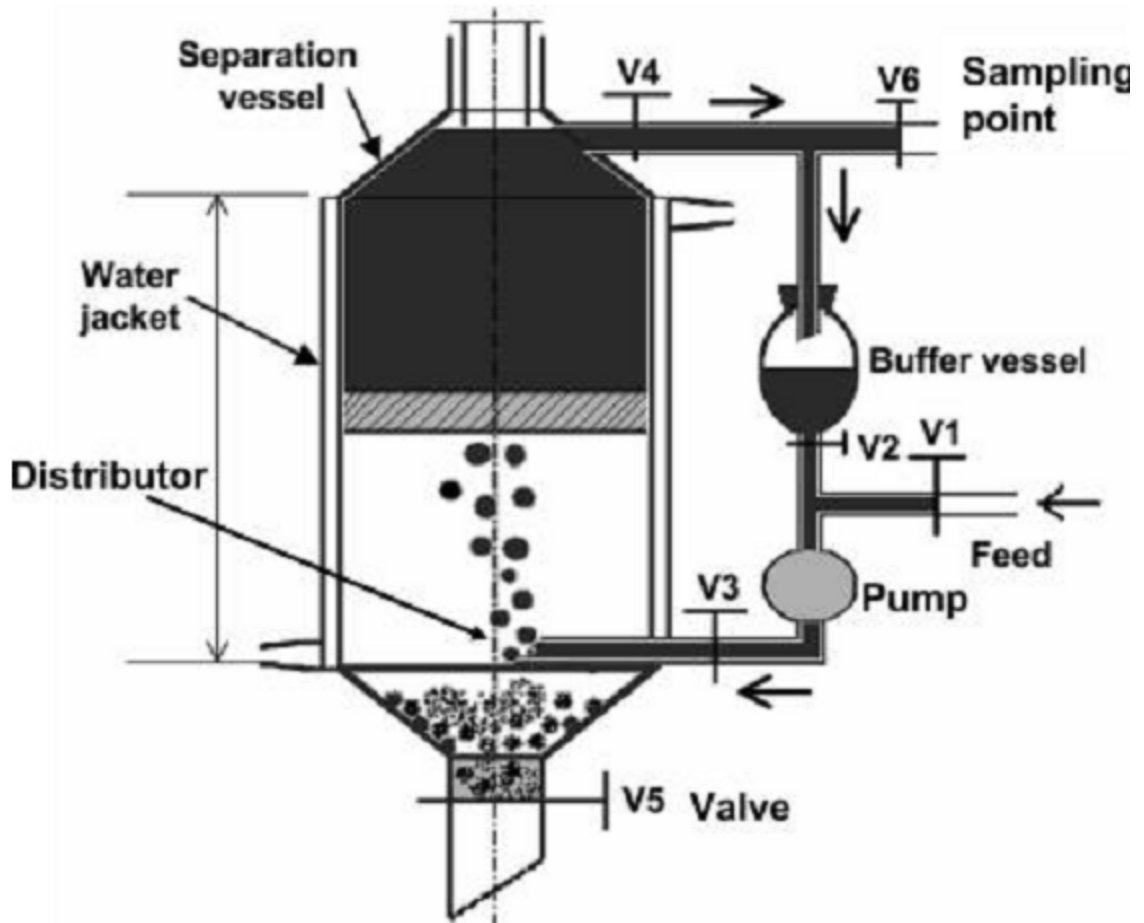
Figure 1-11: Experimental setup utilized by Gu et al. (2007) for washing naphthenic froth with water.

Gu et al. (2007) was able to produce two very different rag layers at two different N/B ratios, 7 and 0.7. At N/B = 0.7, the rag layer was observed to be unstable and deposited to the bottom of the vessel upon gentle agitation. However, at higher N/B ratios the rag layer was observed to be much more dense and viscous, remaining stable after gentle agitation.

The N/B ratio is very important since it has been shown to influence the rigidity or flexibility of an oil-water interfacial film. A critical N/B ratio is often described where values below the critical ratio produce films that are rigid and at ratios above, the interfacial film is observed to be flexible. For commercially used naphtha the critical ratio is approximately 4, (Wu 2003; Yang and Czarnecki 2002;Yeung et al. 2000). These more detailed/ controlled studies correlate well with the observations of Gu et al. (2007).

To collect the rag layer which had formed at N/B=0.7, first the solids which had accumulated during the washing period are removed from the bottom of the vessel. After that, the rag layer is gently agitated so that it settles to the bottom of the vessel. The settled rag layer is removed from the cone-shaped outlet at the bottom.

To remove the rag layer formed with N/B = 7, municipal water is flowed into the vessel enabling the organic phase to overflow. As water begins to overflow pumping is ceased, with the remaining water released through the bottom outlet. After complete removal of water, the rag layer is collected from the bottom of the vessel.

The most common laboratory method used to form a rag layer includes emulsification of water in a sample of diluted bitumen or froth, followed by gravity separation of the emulsified water from the diluted organic phase (settling or centrifuging), (Czarnecki et al. 2007; Saadatmand and Yarranton 2008; Jiang et al. 2007; Jiang et al. 2008; Jiang et al. 2011). In the current study, samples are emulsified by shaking, with a rag layer formed after sufficient separation time.

1.7.   SOLUTIONS TO RAG FORMATION

Chemical aids added to the process could change the amount of the rag layer produced. Some studies have been carried out to understand the effect of different chemicals on the amount of the rag layer produced. Understanding these effects help with choosing the right additives for the different type of ores.

Certain chemicals can reduce association of solids with organics by altering the solids double layer and charge. As previously discussed, the rag layer contains oil-wet clays associated with oil precipitates such as asphaltenes. One of the approaches used to break the rag layer is to use chemical aids to make clays less oil-wet. In bench-scale studies, sodium metasilicate ($NaSiO_3$) addition was observed to disperse the clay solids and minimize bitumen-clay coagulation by changing the double-layer Also, the addition of sodium metasilicate and sodium hydroxide increases the pH and emulsifies oil and separates it from solids by converting the present naphthenic acids to oil soap which emulsifies oil and separates it from solids, (Jiang et al. 2007; Jiang et al. 2008; Jiang et al. 2011).

In other studies Czarnecki et al. (2007) studied how using different types of demulsifiers can increase or decrease the amount of the produced rag layer. Demulsifiers are surface active material that readily adsorb at an oil-water interface due to their amphiphilic nature and they are used to improve water removal. In oil sands processing, demulsifiers are introduced at the froth treatment stage prior to gravity separation. In emulsion treatment and separation there are two types of demulsifier. Type F as referred to by Czarnecki et al. (2007) improves separation through flocculating water droplets to form larger aggregates that settle faster. Type C demulsifiers improve separation by increasing the coalescence efficiency between colliding droplets. The two demulsifiers are somewhat different chemically. Type-F demulsifiers are high molecular weight, 'sweeping' and gathering the fine droplets in the emulsion, while the Type-C demulsifiers are much more surface active, of lower molecular weight and oil soluble.

The settling speed of flocs and droplets in a settling vessel is related to their density difference with the continuous phase. From experimental examination Czarnecki et al. (2007) found that with the flocculant Type-F additive, the flocs formed have a relatively low density and may travel to a separator overflow. This mostly happened at higher concentration of the additive compared to the lower concentration. However, type-C demulsifiers form water droplets which settle down at an acceptable rate as a result of their size and density and would not travel to the overflow stream. As a result, type-C demulsifiers are suggested in systems with the rag layer problem, (Czarnecki et al. 2007).

1.8. OUTLINE OF THESIS

This work is intended to improve our understanding of rag layer formation. A detailed study on the rag layer emulsion and its associated solids will be conducted and compared with a similar sample which shows no capability to form a rag layer.

CHAPTER ONE: The chapter began providing a high-level overview of the oil sands industry and the bitumen production process. It was briefly discussed that the formation of a rag layer during froth treatment could lead to fouling in upgrading. A detailed discussion on previous rag layer studies is provided, highlighting their observations and opinions regarding rag layer formation and destabilization. The discussion is extended to consider the individual components that contribute to the formation of a rag layer.

CHAPTER TWO: Chapter two discusses the experimental practices used throughout the study. Details on the laboratory technique used to form a rag layer are also provided, along information on the two extracted froth samples.

CHAPTER THREE: Chapter three includes the experimental results. The two froth samples are studied in parallel with comparisons continually made to better understand the key properties that lead to rag layer formation. Solids are extracted from the two froth samples are thoroughly experimented to reveal their role in rag formation.

CHAPTER FOUR: Consideration of the experimental data is made to form a reasonable conclusion on the key properties that contribute to the formation of a rag layer. Details on the future work and how such work can support current findings are presented.

2. MATERIALS AND EXPERIMENTAL METHODS

2.1. FROTH SAMPLES

Formed rag layers are problematic when trying to separate two liquid phases. In unconventional oil recovery (oil sands) these formations are frequently observed during froth treatment; in the inclined plate settler, and the primary and secondary cyclones, with the secondary cyclone rag layer often considered being the most troublesome. In the current study, two samples (1L) were used as received from the CNRL froth treatment plant. Images of those settled samples and their points of removal from the froth treatment process are shown in Figure 2-1. All samples were recovered from the froth treatment processing plant while it was experiencing difficulties with rag layer formation.
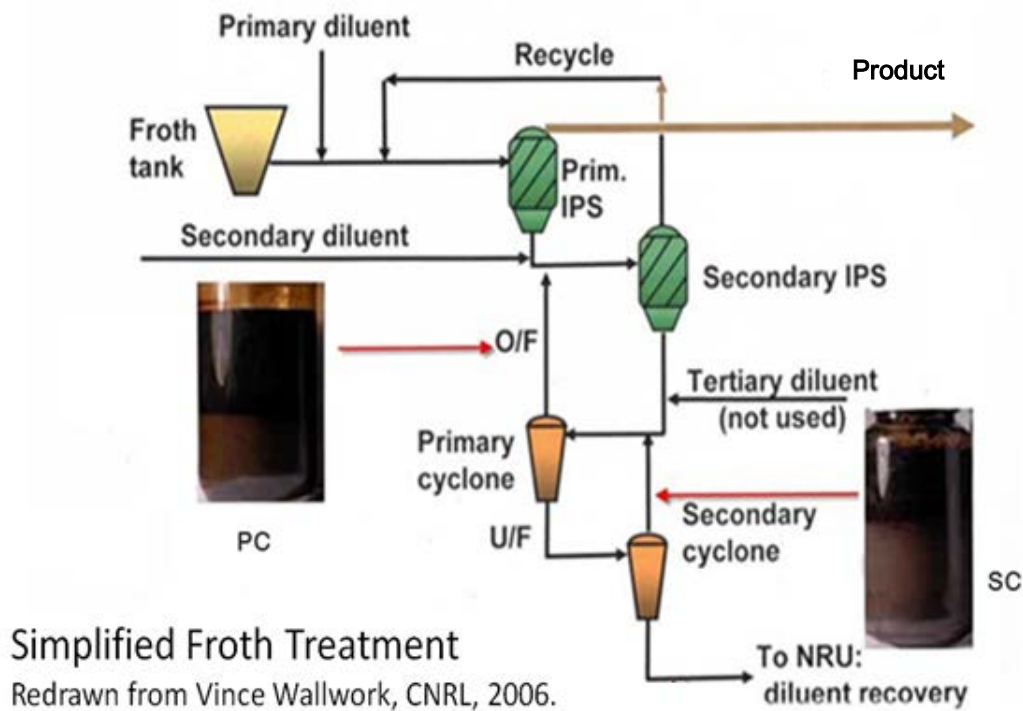
Figure 2-1: Schematic of the froth treatment process and the specific locations where samples were removed, (Masliyah 2009).

Throughout the thesis the following acronyms will be used to describe the primary cyclone overflow [PC] and the secondary cyclone overflow [SC].

Figure 2-2 shows both PC and SC samples in their settled state. Both samples show separation of the oil and water phases, with the water phase 'clouded' by dispersion of fine particles. At this point it is important to note that even though both samples appear to be similar, it is only the SC sample that forms a rag layer. Hence, our study compares in-detail both samples to better understand the key properties, chemical and/or physical, that lead to the formation of a stable rag layer.
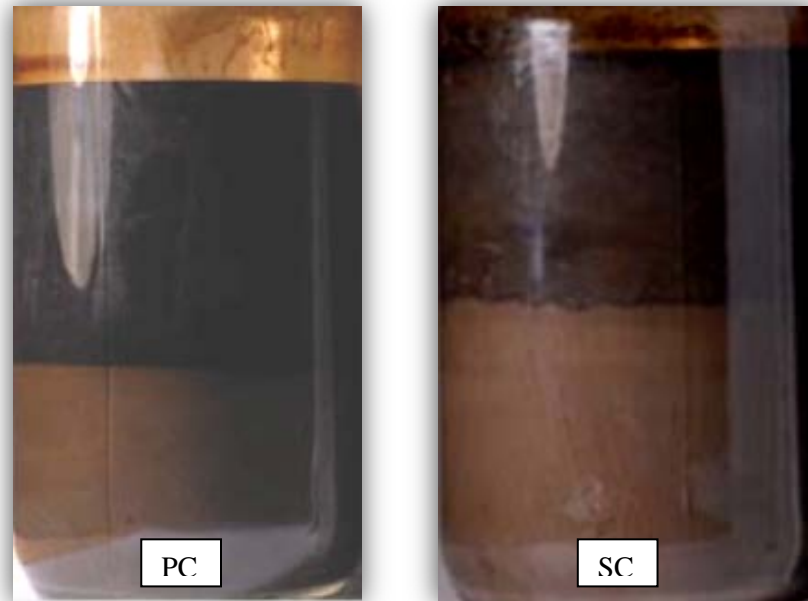
Figure 2-2: (LHS) Sample from primary cyclone overflow (PC); (RHS) Sample from secondary cyclone overflow (SC).

2.2. EXPERIMENTAL METHODS AND SAMPLE PREPARATION

Since the as received samples had separated showing no rag layer formation, a trial and error protocol was established in an attempt to rebuild a stable rag layer. The protocol was based upon the fact that the samples were from a time of process during which rag layer was a problem. This eliminated the need of centrifuging which has been used in earlier studies for rebuilding the rag layer as the samples readily reproduce a rag layer upon agitation. Through trial and error it was found that the thickest and most stable rag layer is obtained when the diameter of the container is small. If the rag layer was building

in a wide container, it would have been less thick. That means, if the rag layer was produced in a wide container, by tilting the container the rag layer moved easily along with all other phases. But the rag layer made in the narrow cylinder does not move. Also the best method to collect the rag layer is to use a spatula. If pumps, pipettes and other suction methods were used to collect the rag layer water from water phase penetrated the rag layer.

Samples were first homogenized using a mechanical shaker (10 minutes, 170 strokes/min), followed by 20 minutes at a lower speed (85strokes/min). Samples were then transferred to a sealed 100 mL glass cylinder and allowed to settle for 14 days. At day 14 the content of the cylinders was shown to have separated into four fractions:

1. The solids free, solids-free oil layer
2. Rag layer
3. Water phase
4. Coarse solid sediment

For analysis, each fraction was carefully removed using a narrow tip pipette (oil and water phases), with the rag layer removed with a spatula.

The collected samples were then analyzed to determine:

- Water and solids content
- Sample density
- Physical appearance under a microscope
- Emulsion continuous phase

As discussed in chapter 1, solids and fines play a significant role in emulsion stability. Hence, the solids collected (centrifugation) from each fraction (both PC and SC samples) were extensively characterized using a variety of techniques:

- Particle size analysis –dynamic light scattering
- Quantification of the toluene insoluble organics adsorbed on the solids using thermal gravimetric analysis (TGA)
- Particle wettability - film flotation
- Particle mineralogy -X-ray diffraction (XRD)

- Determination of surface functional groups – Fourier transform infrared spectroscopy (FTIR)

2.2.1. DENSITY

Fluid densities were measured using an Anton Paar density meter (DMA 38). 1mL of sample was injected into the instrument using a toluene-safe syringe. Densities were recorded after the temperature had stabilized at $23^{\circ}C$.

2.2.2. OPTICAL MICROSCOPE OBSERVATION

Microscopic images of each sample were collected using a Carl Zeiss Axioskop 40 Pol microscope. Samples were gently pipetted onto a glass slide with a cover slide placed on top.

2.2.3. EMULSION TYPE – RAG LAYER

While there is much interest in rag layer formation, there remains much discussion on whether or not these formations can be described as an emulsion, and if they can, what type of emulsion forms? In the current study, rag layer droplets were injected into milli-Q water, naphtha and toluene to determine the continuous phase using a syringe with a needle with a blunt end and 1 mm width, gauge 19. The diffusional characteristics of each droplet were studied by examining images captured consecutively using the image software of the KRUSS drop shape analyzer, see Figure 2-3.

The syringe was placed inside of the syringe-holder and a container holding either water or naphtha was placed in front of the light source and the camera lens. Samples were slowly injected to identify whether or not a stable droplet would form or immediately diffuse through a complementary phase.
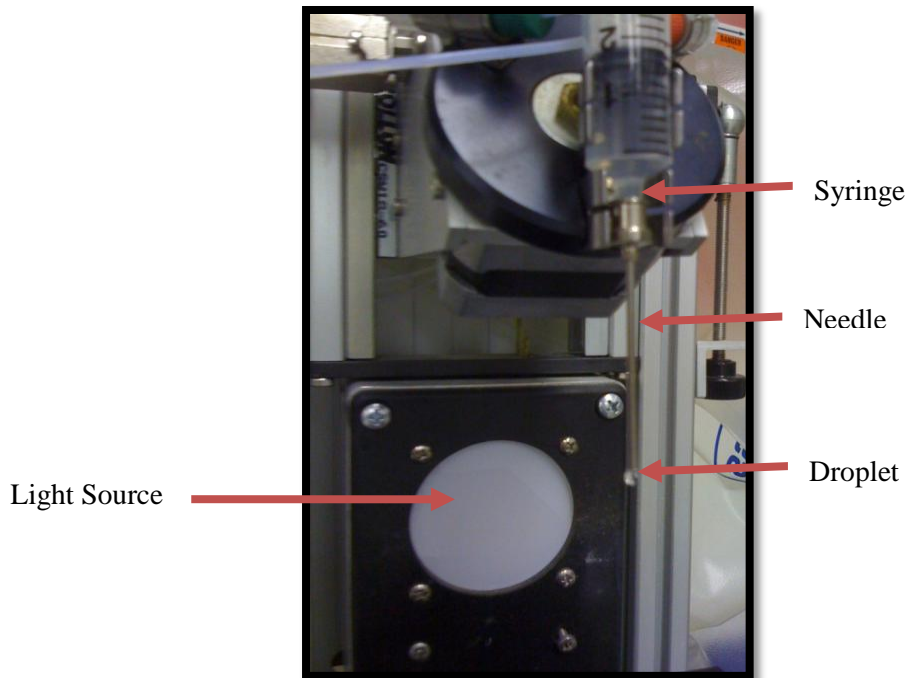
Figure 2-3: Drop shape analyzer setup.

2.2.4. WATER CONTENT

Water content was measured using Karl-Fischer titration. Analysis was conducted on 0.2 µL sample.

2.2.5. SOLIDS EXTRACTION AND CONTENT MEASUREMENT

Solid samples from all fractions in the settling column were collected and washed with toluene before centrifuging at 20,000g for 25 minutes. The centrifuged samples were separated into three phases; i) an organic top phase, ii) a thin water phase and iii) solid sediment. The two fluids were carefully decanted using a narrow tip pipette; whilst the remaining sediment was re-dispersed and washed again with fresh toluene to remove any bituminous impurities. Samples were shaken using a vortex mixer and sonicated for 30 minutes before repeat washing with toluene. Sample washing continued until the supernatant appeared clear, with all loose and soluble organics removed from the solid surface (only insoluble organic matter remain). The washed solids were dried in a

vacuum oven for 24 hours to vaporize all solvents. A mortar and pestle was used to crush the dried cake forming a fine powder.

2.2.6.   THERMAL GRAVIMETRIC ANALYSIS

Thermal gravimetric analysis was conducted using an STA 409 PC Luxx thermal analyzer, Netzsch Instruments. Dried solids were heated for 4 hours from room temperature to 700 ^{o}C at 5°C/min to reveal their organic content. 7 mg of solids was used for each test.

2.2.7.   MEASUREMENT OF WETTABILITY BY FILM FLOATATION

To measure solids wettability the film flotation technique developed by Fuerstenau et al. (1991) was used. In this technique the surface tension of the solids, referred to as critical surface tension, is determined by measuring the highest surface tension of a liquid which completely wets the solids. When a solid particle is completely wet by a liquid, it will sink down in that liquid. In this technique solids are sprinkled on the surface of a liquid, usually a water/alcohol solution. If all solid particles in a batch of solids are of the same size and shape, they all have the same critical surface tension. But since the solids are different from one and other they will have different critical surface tensions. By changing the content of alcohol in water a wide range of surface tensions are obtained for the liquid and the critical surface tension of all solids in one batch could be measured.

By measuring the weight of sinking solids, the cumulative mass fractions of floating solids on surface of liquids with different surface tensions are measured. From the experiment the cumulative distribution curve and the frequency distribution, $f_i(\gamma_c)$, of critical surface tension of solids are derived.

The mean critical surface tension is calculated from frequency distribution curve using the following equation:

$$\overline{\gamma}_c = \sum (\gamma_c)_i f_i(\gamma_c) \qquad \text{(2-1)}$$

where; $\overline{\gamma}_c$ is the mean critical surface tension, γ_c is the critical surface tension for f_i floating mass fraction of solids, (Fuerstenau et al. 1991;Trong et al. 2009).

Considering the theory explained, the film flotation technique is explained below:

A schematic of the experimental setup is shown in Figure 2-4. A glass dish (l=120mm, w=50mm,h=20mm) with a glass ring attached at one end(diameter = 50 mm) was used to retain the solution and contain the floating solids. An aluminum weighing dish was placed under the glass ring to collect any sinking solids. Increasing concentrations (0-100%) of ethanol in water solutions were prepared, to lower the surface tension from 72 to 22mN/m. The glass container was filled with the desired ethanol/water mix and a weighing dish placed under the glass ring. Solids were measured to 0.012g and sprinkled carefully on the air-water interface within the glass ring. Solids collected in the measuring dish were measured after 4 minutes. To determine the mass of the deposited solids, the solids plus weighing dish were dried in a vacuum oven at 50°C for 24 hours. The percentage of floating solids is then plotted against surface tension to obtain the cumulative distribution curve and calculate critical surface tension. With this technique it is possible to compare the wettability of two batches of solids and determine which one is showing more hydrophobic behavior. More hydrophobic solids have a lower mean critical surface tension, (Fuerstenau et al. 1991; Trong et al. 2009).
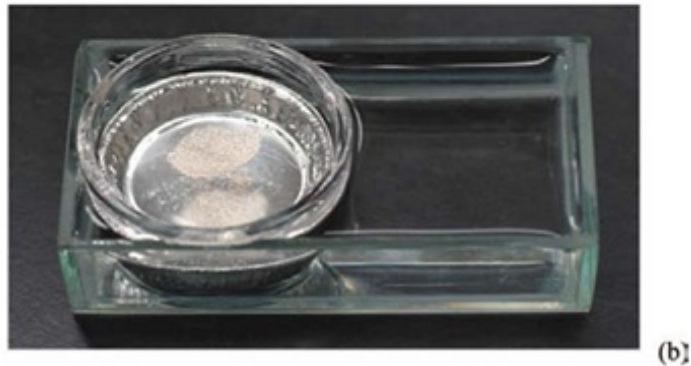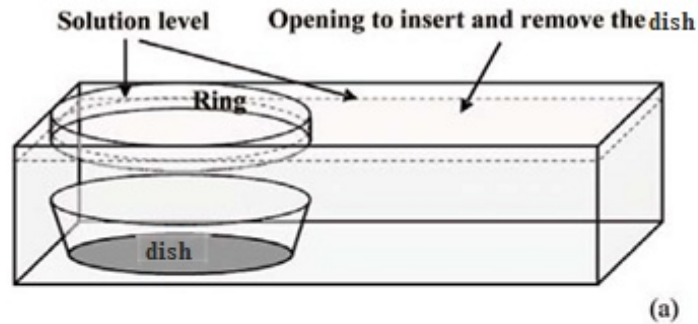
Figure 2-4: Film flotation setup by Trong et al. (2009)

2.2.8. REMOVAL OF ORGANICS BY LOW TEMPERATURE ASHING

It is necessary to remove the insoluble organic matter from the solids prior to particle size and X-ray. Low temperature ashing (LTA) was used to remove any insoluble organic matter on the solids. LTA uses radio frequency radiation to excite oxygen molecules to remove organic matter from the solids, (Adegoroye et al. 2010; Adegoroye et al. 2010; Adegoroye et al. 2010). A plasma asher (K1050X, Quorum of Kent) was used for this purpose. The process is carried out under vacuum pressure of 0.6 mbar to enable removal of any combusted organics.

Dried solids were placed in glass Petri-dishes and loaded into the LTA. The equipment evacuates all gases present in the reaction chamber and introduces oxygen. RF was applied to the system at a power of 50 W for 150 minutes. After the first run, samples were stirred so that all surfaces of the solids were exposed to the radiation. The process was repeated until the weight loss becomes negligible.

2.2.9. FOURIER TRANSFORM INFRARED SPECTROSCOPY

Solids infrared spectra were obtained by a Biorad FTS 6000 from CSM Instruments. KBr was used as the background salt with samples mixed to a concentration of 2.6wt.%. Mixtures were placed on the sample holder for absorbance measurement.

2.2.10. PARTICLE SIZE DISTRIBUTION

Particle size analysis was completed using a Malvern Mastersizer 2000 (dynamic light scattering). This instrument uses laser diffraction to measure the particle size distribution. The particles passing through a laser beam will scatter light according to their size. Solids that were collected according to 2.2.5 had formed a cake and were dispersed prior to measurement to allow accurate measurements of the primary particle size. Since the results obtained with this method are influenced by the dispersion condition of solids in water, it is very important to ensure that solids are fully dispersed and in their primary size prior to the experiment.

Suspensions were prepared to a concentration of 0.004 g/mL solids in milli-Q water. 3-4 droplets of a sodium silicate solution was added to the suspension and then sonicated for 30 minutes. Sodium silicate was added since it is a known dispersant for particles.

The sodium ions replace calcium and magnesium ions on surface of clays, creating a charge effect which causes particles to repel one another and prevent aggregation. .

2.2.11. X-RAY DIFFRACTION ANALYSIS, XRD

It is common to analyze the mineralogy of solid samples according to their size fractions. In this study, most samples were smaller than 3 μm. Distilled water was added to the samples before shaking with a Vortex Mixer. The sample was then transferred onto a glass slide with use of pipette. The slide was placed on a hot plate at low heat until the sample was dried and then XRD was run. Since swelling clays such as smectite were suspected, a slide must be analyzed also after it was glycolated. For that, the slide was placed in a glycol vapor bath overnight and the test was run again on the glycolated clays.

3. RESULTS AND DISCUSSIONS

3.1. INTRODUCTION

In this chapter the two overflow samples recovered from the primary (PC) and the secondary cyclones (SC), are examined using the experimental techniques previously described.

3.2. SETTLING TESTS

Following the procedure outlined in Section 2.2 – reforming the rag layer, samples PC and SC were allowed to stand for 14 days. Figure 3-1 shows images of the two settling columns (PC and SC) after 14 days. Clearly, the PC sample did not form a stable rag layer, while the SC sample formed a rag layer that would remain stable for a much longer time period (in excess of ten months). It should be mentioned that the PC sample separated immediately after mixing with no visible rag layer formed. After separation the PC sample formed three distinct regions; i) solids-free oil layer, ii) cloudy water phase (solids dispersed) and iii) solids sediment. In comparison, the SC sample formed a significant rag layer, with a thin layer of solids-free oil layer, a cloudy water phase (solids dispersed) and a sediment bed below the rag layer. For each sample the solids-free oil layer was collected with a narrow-tip opening pipette. The rag layer (only SC) was then gently removed using a spatula, taking care not to disturb or break-down the rag layer structure. After removal of the organic phase the water phase was decanted. Once removed, experiments were completed to determine the type of emulsion formed in the rag layer.
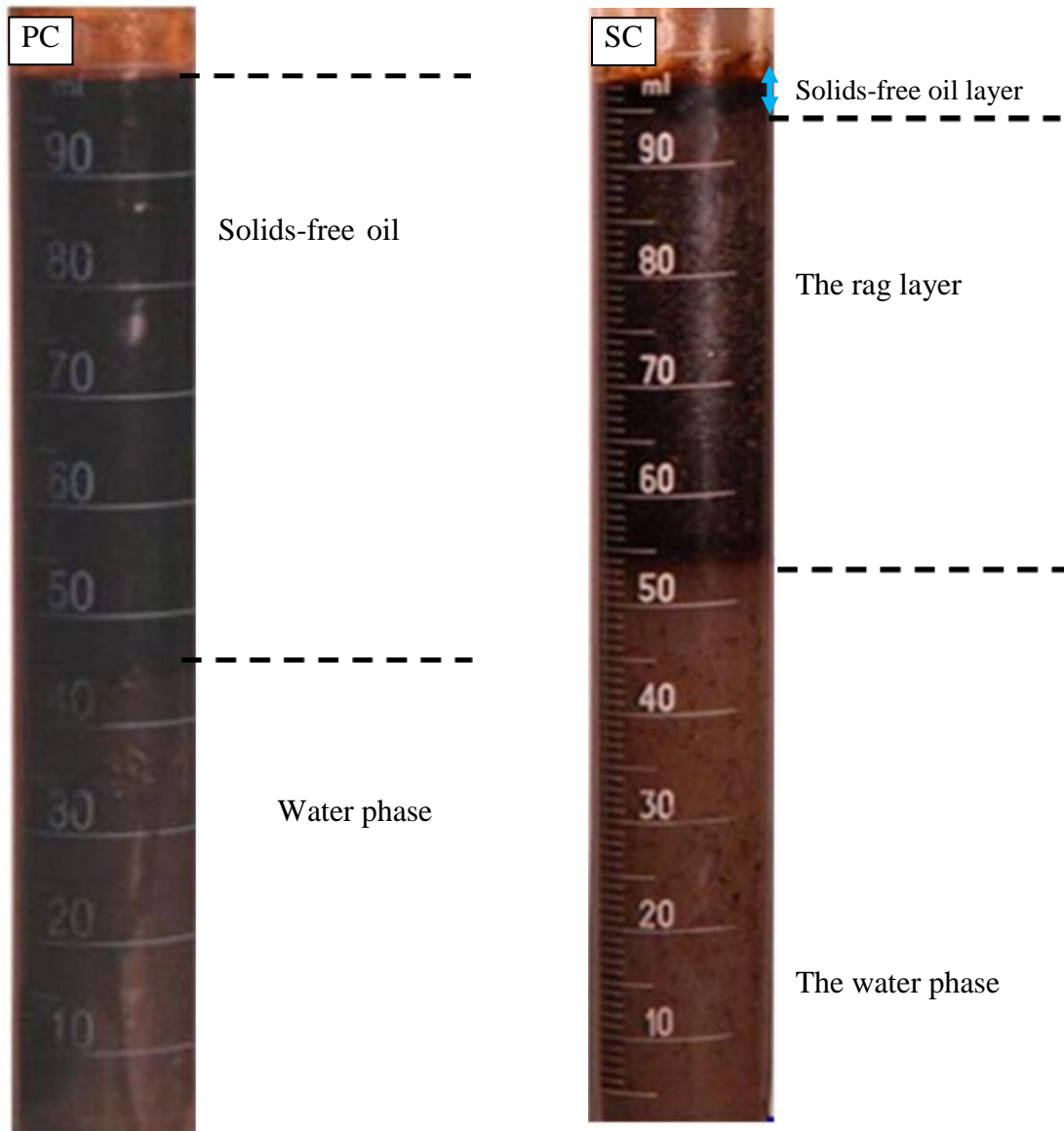
Figure 3-1: Images of the cylinders used for experiments, the one on the left is PC and the one on the right is SC

3.3. DETERMINING THE CONTINUOUS PHASE OF THE RAG LAYER EMULSION

According to Czarnecki et al. (2007) and Varadaraj and Brons (2007) the formed rag layer is an emulsion. To determine the type of emulsion formed, two experimental procedures were used.

First, a small sample of the rag layer was placed at the base of either a water (Milli-Q) or toluene bottle to determine the diffusion characteristics and hence the rag layer continuous phase. Figure 3-2 shows the two bottles immediately after rag layer addition. In the case of toluene, the rag layer immediately diffused through the organic phase, while addition to water resulted in the rag layer droplet floating to the air-water interface and spreading. The two bottles were then shaken to observe the rag layer material under gentle agitation. In toluene the rag layer completely diffused throughout with solids observed to slowly settle, see Figure 3-3. After a period of time the resultant toluene solution was observed to be clear.
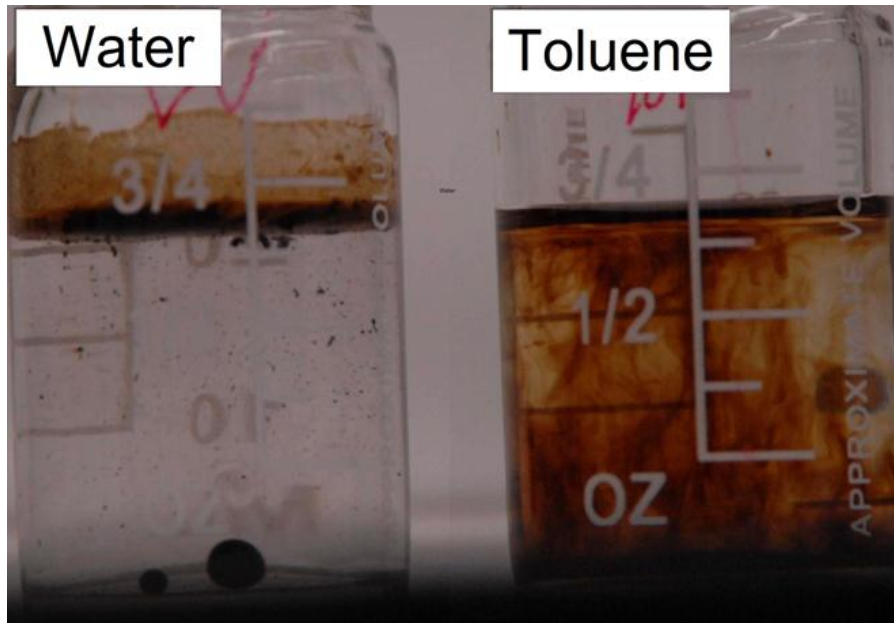
Figure 3-2: Behavior of the rag samples in different solvents. Bottle on the left holds mili-Q water and the right is holding toluene.
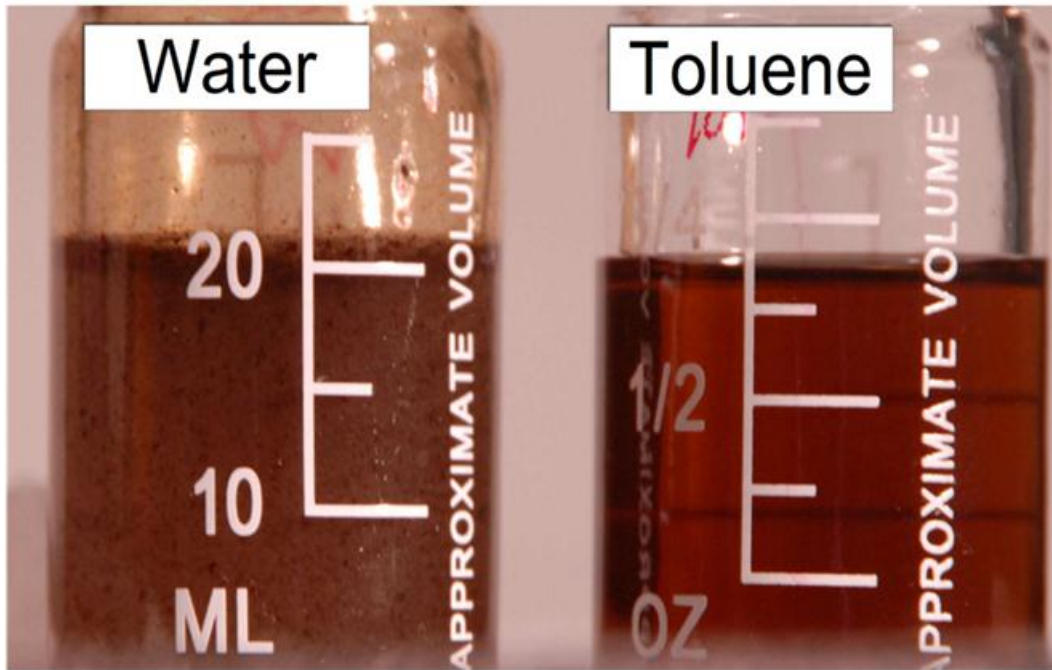
Figure 3-3: Top: Bottles after shaking. Bottle on right: The clear solution obtained from shaking the toluene bottle. Bottle on left: The dispersion obtained from shaking the water bottle. Bottom: Small solid particles from the rag layer, which have settled to the bottom of the toluene bottle.

As the rag layer sample was shaken in water, the rag layer sample was observed to break down and appeared to disperse in water. Over time two liquids phase separated and the rag layer solids began to collect in the thin oil layer above the water, see Figure 3-3.

These observations confirmed that the rag layer is a continuous oil phase emulsion, and that the solids present in the rag layer are predominantly hydrophobic.

DETERMINATION OF THE CONTINUOUS PHASE OF EMULSION WITH A DROP SHAPE ANALYZER (DSA)

To confirm our previous observation, a similar experiment was conducted using a droplet shape analyzer, gradually injecting a droplet of the rag layer into either water or naphtha. Using the tensiometers' microscopic camera it was possible to observe the real-time mechanics of droplet mobility or diffusion. Section 2.2.3 describes the experimental procedure.

Figure 3-4 and 3-5 show images taken by the DSA 16. The black rectangular shape observed in these images represents the needle of the syringe from which the rag layer was injected into the solvents.

Figure 3-4 shows images of the rag layer gradually being injected into naphtha. Clearly, gradual injection into naphtha does not allow the formation of a stable droplet, with the rag layer droplet being readily dispersed. The color of naphtha also became darker as the rag layer was further injected into the solvent.

However, rag layer injection into water (Figure 3-5) shows the clear formation of a droplet-shape, indicating an immiscibility of the two fluids. After the rag layer droplet-shape detaches from the needle the fluid and its dispersed solids float to the air-water surface. This study reaffirms our initial finding.

By comparing the rag layer behavior in different solvents, the rag layer is found to be incompatible with water but has high affinity for oil solvents. From these images, it is understood that the continuous phase of the rag layer is oil.
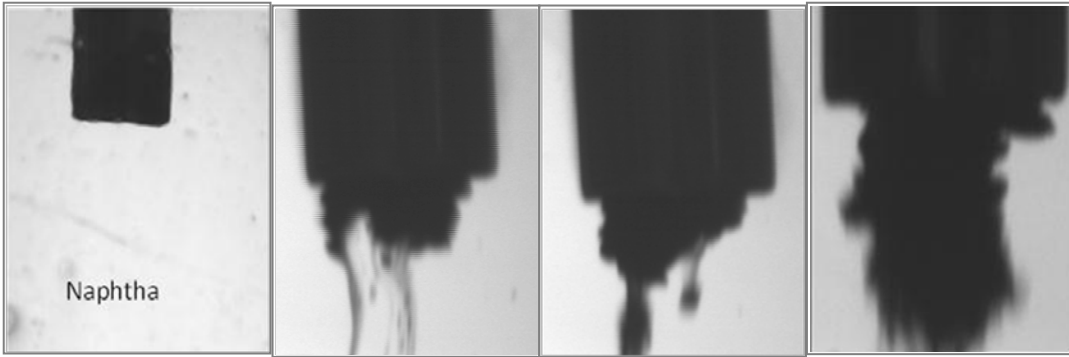
Figure 3-4: The attempt to create a rag layer droplet-shape in naphtha.
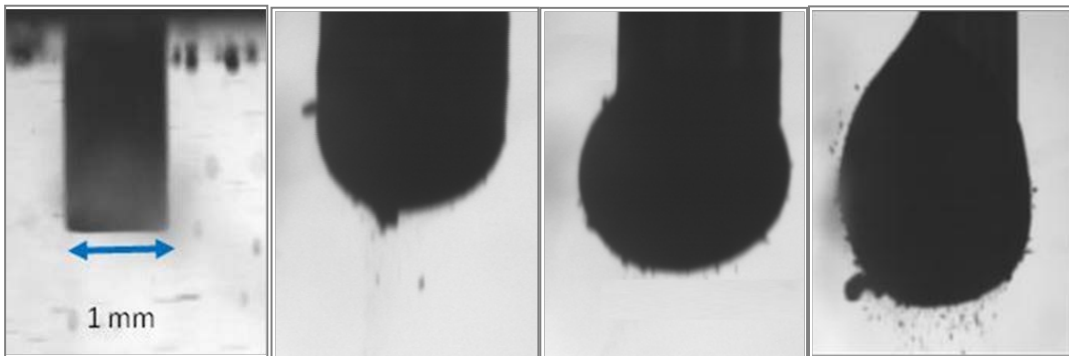
Figure 3-5: A rag layer droplet-shape created in water.

3.4. OPTICAL MICROSCOPE OBSERVATION

Microscope image from the separated oil phase is shown in Figure 3-7 and the rag layer in Figure 3-8. In the solids-free oil layer small water droplets (diameter ~3-7μm) are clearly identified to be dispersed throughout the continuous oil phase. This observation is similar to previous images of water-in-diluted bitumen emulsions shown by Feng et al. (2009) shown in Figure 3-6. From this similarity it is understood that the water in oil emulsion formed in the solids-free oil layer phase is not a complex emulsion.
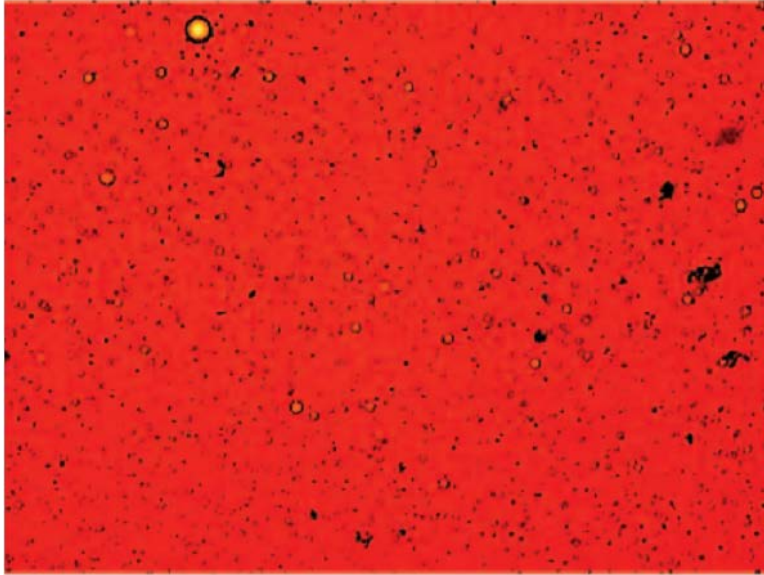
Figure 3-6: Image of water-in-oil emulsion presented by Feng et al. (2009)

For the rag layer samples shown in Figure 3-8, clear identification of water droplets is far more challenging. The dense and complex nature of the rag layer is reasonable if you consider the images presented in chapter 1. In an attempt to separate the rag layer components white circles have been drawn around several water droplets, green circles around material that we will refer to as solid black masses and yellow and light blue circles around areas that appear light and dark brown in color, respectively. The solid black masses and the brownish area are of unknown nature. It is suspected that they are flocs of water droplets and solid particles with precipitated asphaltene.

It was understood in previous sections that the continuous phase of the rag layer is oil. Since those images are very complex and dark, the rag layer was diluted with either heptane or toluene in an attempt to see the structure more clearly. Dilution of the sample was completed on the microscope slide with diluent added drop wise until the solvent ran clear.

Figure 3-9 shows a rag layer diluted with heptane. Clearly, there are no major differences from the un-diluted sample, with the spherical water droplets and murky regions still remaining.

However, Figure 3-10 is an image of the rag layer after excessive dilution with toluene. Addition of toluene has a significant effect, as would be expected based on the previous

observations in Section 3.3. The dark brownish regions seem to have been removed, clearly exposing the water droplets and the solid black masses that remain.

These two experiments, dilution with heptane and toluene, have confirmed that part of the rag layer (dark brown regions) is soluble in toluene and not heptane (i.e. soluble in solvents with high aromaticity), while the black masses appear insoluble in both solvents. It is speculated that the black-masses perhaps consist of flocculated networks of fine solids are water droplets, yet alternative experiments will be needed to verify such belief.

By studying the solids found inside in the rag layer, it may be possible to validate our current hypothesis which considers the solid black masses to be flocs of water droplets, solid particles attached to each other by organic materials.
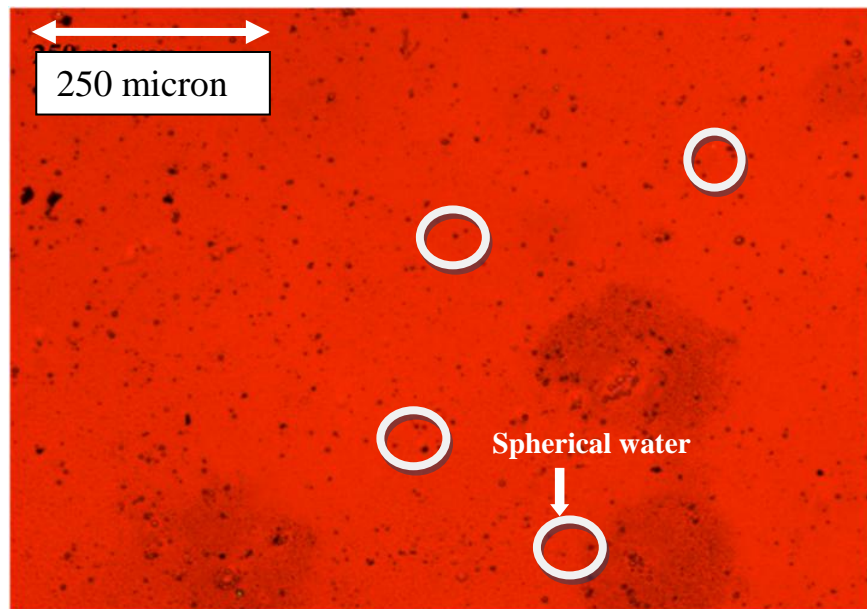
Figure 3-7: Water-in-oil emulsion formed above the rag layer
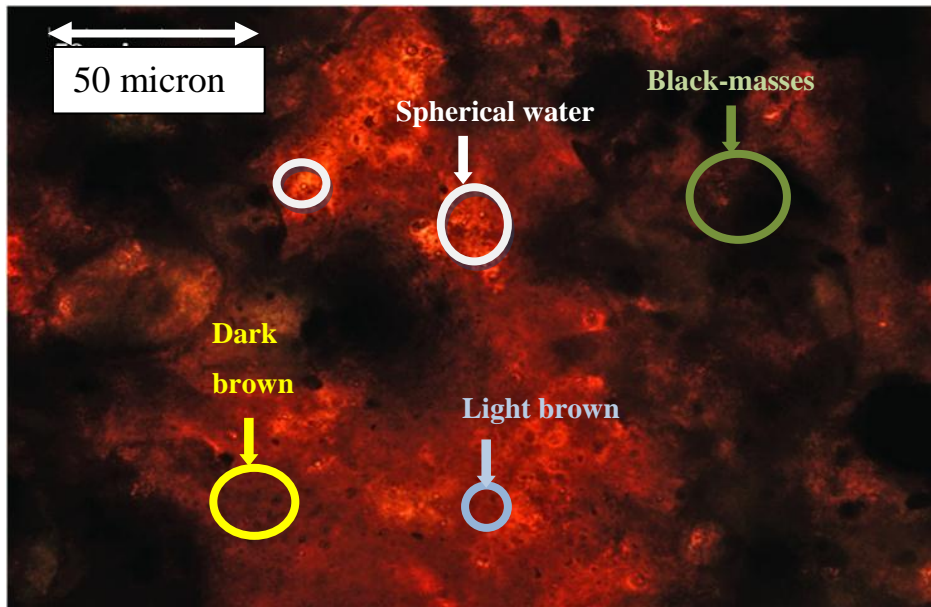
Figure 3-8: Microscopic image of the rag layer
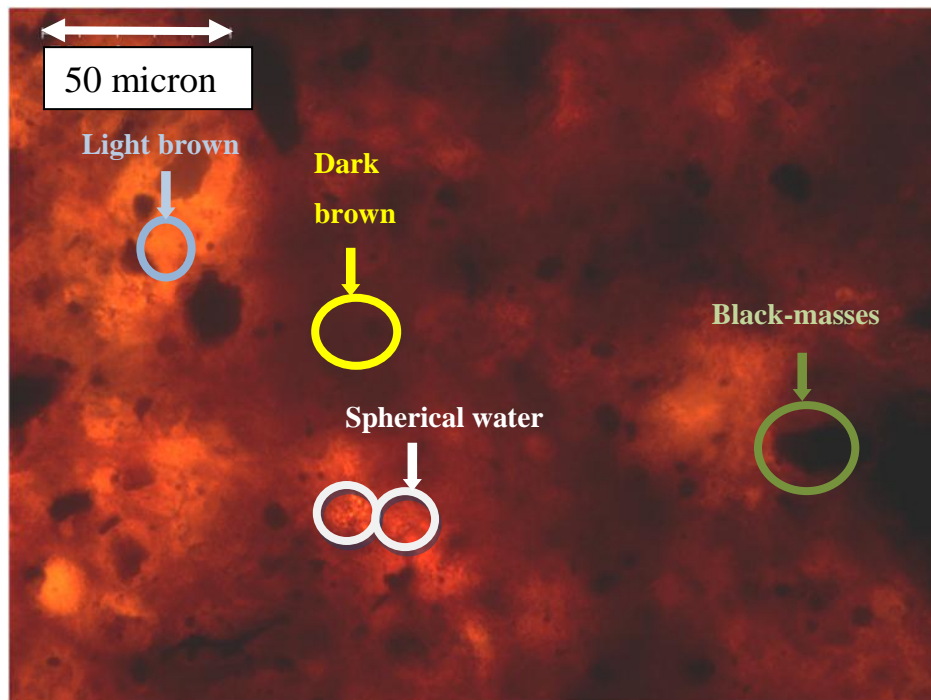
Figure 3-9: The rag layer sample diluted with heptane
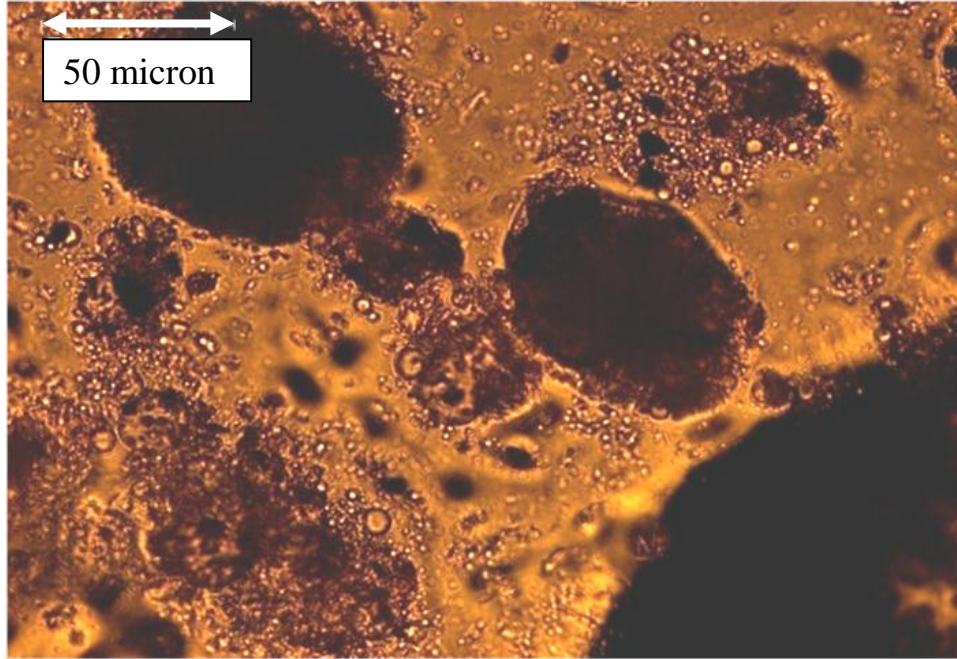
Figure 3-10: A rag layer sample diluted with toluene.

3.5. DENSITY

Samples were collected from different heights along the settling cylinder to include the rag layer if any, and the water and oil phases. The density of each collected sample is shown in Figure 3-11 for both PC and SC samples. A picture of the SC sample is shown as a reference to the sampling positions. For the SC sample, the measured density was observed to gradually increase down the column (top to bottom). Those density changes result from the different phases, i) the solids-free oil layer ii) the rag layer and iii) the cloudy water phase. In the rag layer itself, a density gradient was measured with the sample density removed between 95-70mL equal to 960kg/m^3, and the sample density from a lower position 70-55mL equal to 980 kg/m^3. Such small increases in the rag layer density most likely result from changes in rag layer water content. This will be further discussed in Section 3.6.
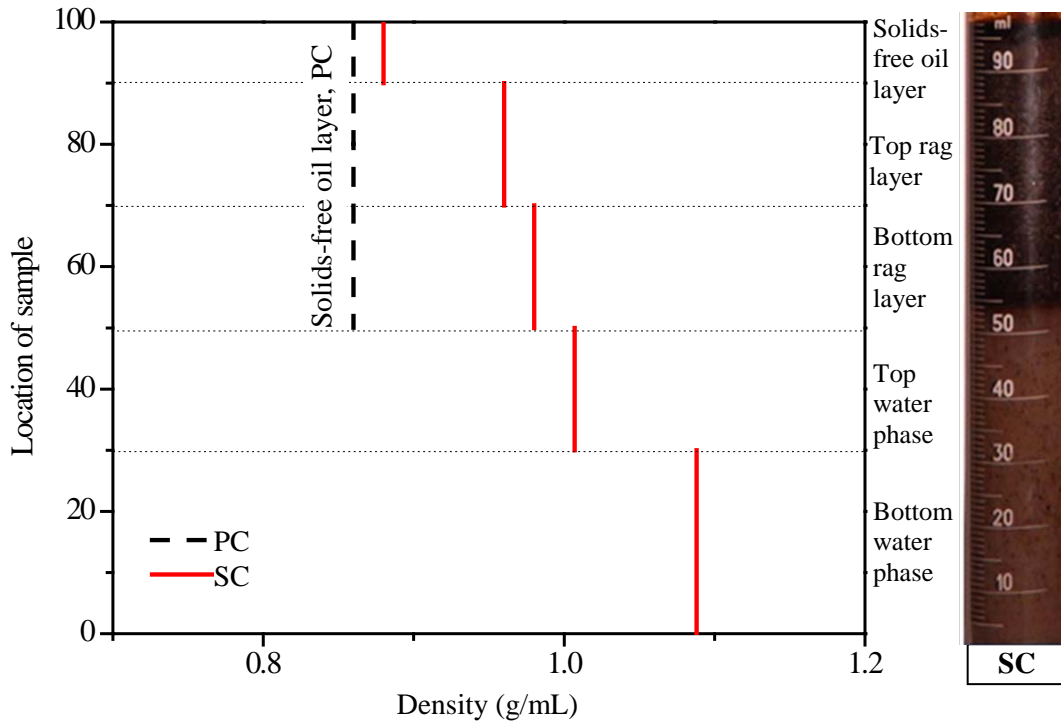
Figure 3-11: Density of PC and SC at different heights

The small solids-free oil layer exhibited the lowest density equal to 880kg/m^3 and the water phase the highest measured densities, see discussion below. With the rag layer density in between the oil and water phases, it reaffirms the discussion around intermediate density as a mechanism to form stable a rag layer, see Section 1.4.2. In the water phase a density gradient was also measured. In the region 50-30mL the sample density was equal to 1010kg/m^3 and increased to 1100kg/m^3 when samples were recovered from a position below 30mL. Clearly this density increase relates to solids stratification throughout the water phase, where fines remain suspended and coarse solids rapidly settle to form a sediment bed at the base of the column.

The density of the oil phase in the PC sample was equal to 860kg/m^3, lower than the density of the oil phase in the SC sample. This difference is believed to relate to water content in each oil phase; this is discussed further in Section 3.6.

3.6. WATER AND SOLIDS CONTENT

Water and solids contents were measured for each of the recovered samples from both PC and SC cylinders after 14 days of settling. Experimental protocols have previously been described in Sections 2.2.4 to 2.2.5. Figure 3-12 shows the water content at different heights along the settling cylinder.

As shown in Figure 3-12, the water content in the SC cylinder varies significantly and potentially continuously from the oil phase to the water phase. In solids-free oil layer the water content is 3.05 wt.%, increasing to 22.3 wt.% in the top region of the rag layer (70 – 95 mL) and further increasing to 28.45 wt.% in the lower region of the rag layer (55 – 70 mL). The change in water content in the rag layer supports our previous experiments which showed a density gradient increase from the top to the bottom of the rag layer.

Unlike the SC sample, the PC sample which does not form a rag layer showed no water content gradient. The water content in the oil layer was equal to 0.46wt.% and did not fluctuate with sample position. With such a low water content, clearly there is no stability and water drop out after the sample has been shaken appears to be uninhibited. Figure 3-13 shows a similar plot but assesses the change in solids content with sample height. The solids-free oil layer for both samples is relatively solids free. For the SC sample, measurements in the rag layer made between 95-70mL and 70-55mL resulted in a solids content of 14.75wt.% and 14.43wt.%, respectively. Hence, the solids content was observed not to change (possibly within experimental error) throughout the rag layer. Considering that there was no change in solids content of the rag layer, the gradient observed in the density must be caused only by the change in the water content throughout the rag layer. The increase in density caused by the water content gradient was calculated and it was realized that the value matches the observed change in density.

In water phase of SC, most of the solids had settled to the bottom 10mL of the SC cylinder. A solids content of 22.35wt.% was observed in the bottom 10mL. The solids content of the entire water phase was 5.43 wt.%, this includes the solids which had settled to the bottom 10mL of SC. This value is comparable to the solids content of water phase of PC cylinder which had a solids content of 5.73wt%. Figure 3-14 shows a cylinder prepared using the SC sample. The image clearly demonstrates the separation of solids from the water phase over a two month period. This also explains why the solids content is much higher at the very bottom of the cylinder.
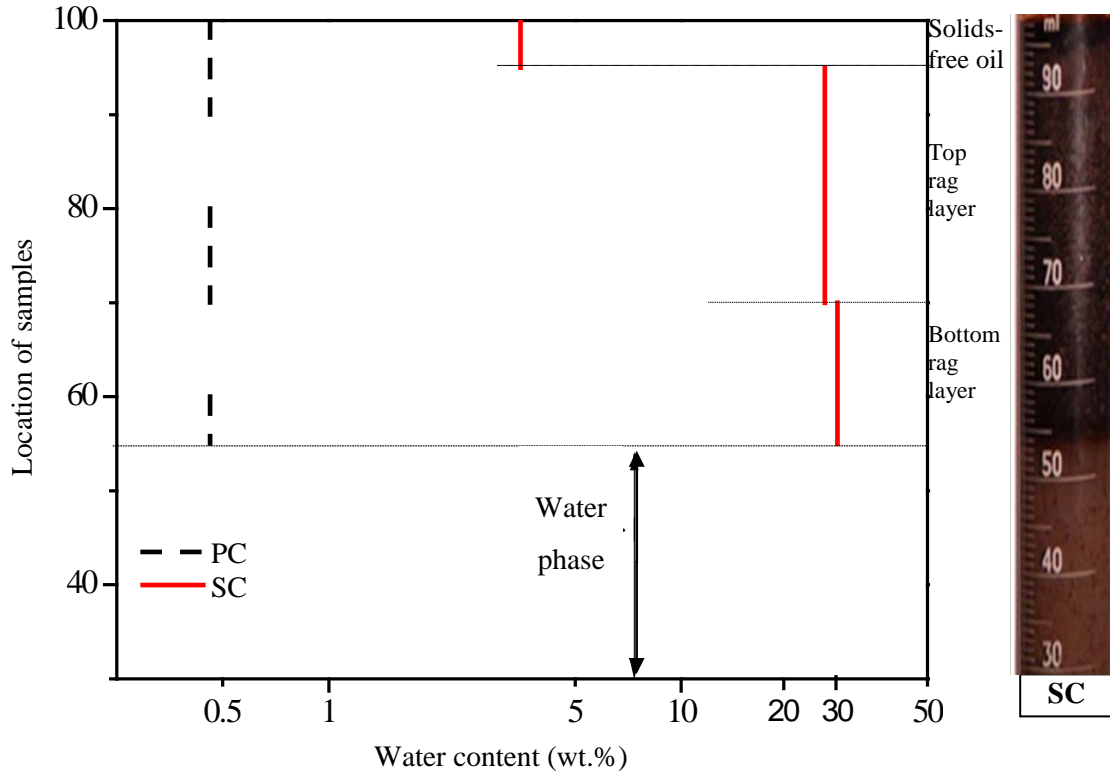
Figure 3-12: Water content of cylinders at different heights.
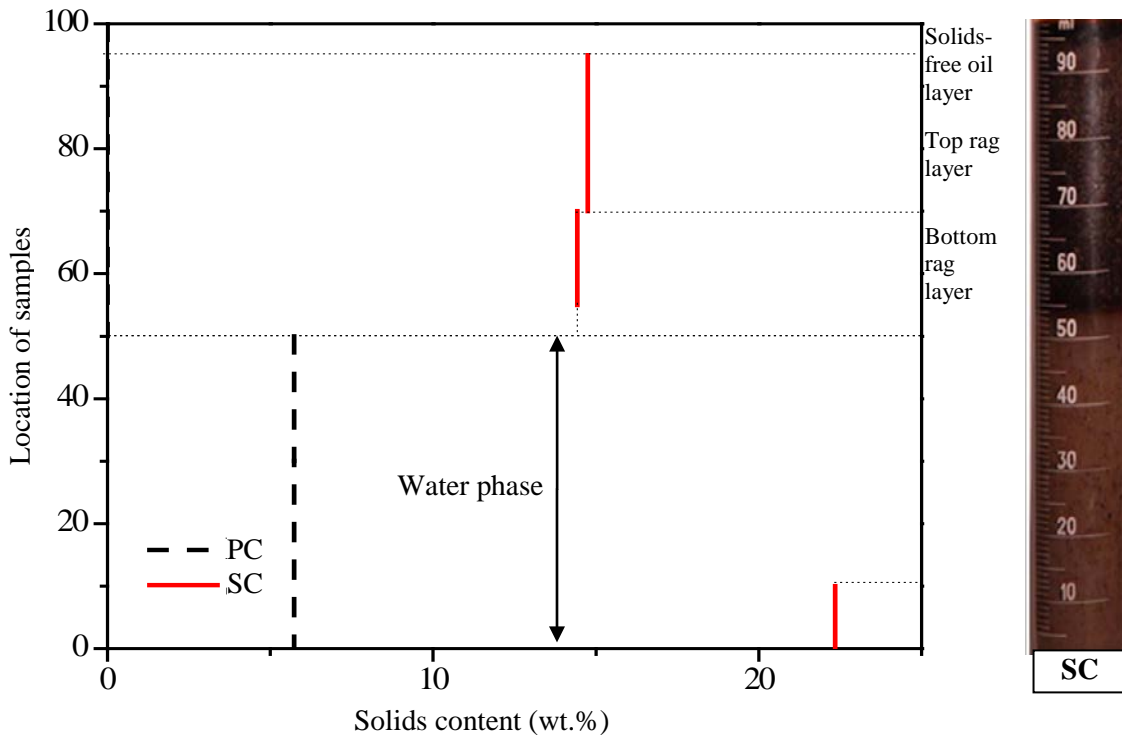
Figure 3-13: Solid content of cylinders at different heights

Figure 3-14: Image of a cylinder prepared from overflow of secondary cyclone after two months. This photograph is taken after the solids dispersed in water phase completely settled to the bottom of the cylinder**.**

3.7. SOLIDS MINERALOGY

Solid particles were extracted from the aqueous phase of both samples and the SC rag layer using techniques previously described in Section 2.2.5. The mineralogical properties of these solids were determined using X-ray diffraction, with the results shown in Figure 3-15.

Abbreviations used in Figure 3-15 and throughout the thesis include:

- Solids in water phase of PC, (PC – Aq. solids)
- Solids in water phase of SC, (SC – Aq. solids)
- Solids in rag layer of SC, (SC – Rag solids)
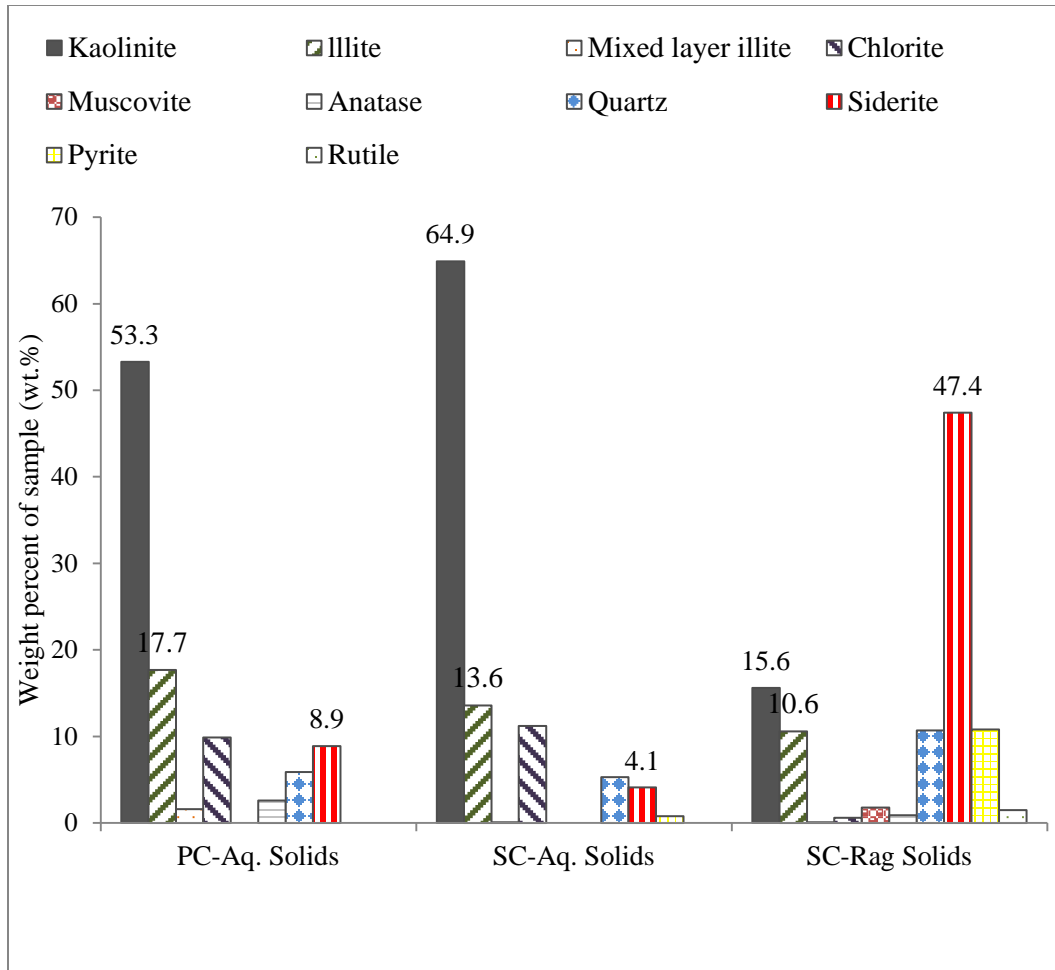
Figure 3-15: X-ray diffraction (XRD) analysis of solids from PC and SC samples.

The mineralogy of PC– Aq. and SC– Aq. solids appears relatively similar. There are some small differences but both samples have significant quantities of kaolinite, similar quantities of illite, chlorite and quartz, and very little if any of mixed layer illite, muscovite, pyrite and rutile.

It seems that the comparison between the Aq. solids and Rag solids is more interesting and potentially provides key information on the main components that result in rag layer formation/ stability. In considering the rag solids there is clearly less kaolinite, but there is significantly more siderite and pyrite. These heavy minerals are much more abundant in the rag layer, with siderite ($FeCO_3$) and pyrite (FeS_2) accounting for 47.4 wt.% and 10.8 wt.%, respectively. This characteristic could potentially underline the key particles that are essential in forming a rag layer.

It should be noted that these heavy minerals do not appear in significant quantities in the PC sample, which has been shown not to form a stable rag layer. The measured diffraction patterns and the calculated patterns for the samples mentioned here are available in appendix.

3.8. PARTICLE SIZE DISTRIBUTION

Particle size distributions of the recovered solids are shown in Figure 3-16. The particle size distributions for the PC-Aq. and SC-Rag solids are almost identical showing a bi-modal distribution. The SC-Aq. sample shows a similar bi-modal distribution, however, the distribution is shifted to the larger particle size and the contribution of coarse to fines (fines < 44μm) on a volume basis is greater. These results appear to be agreement with previous settling tests (Section 3.2) which showed solids in the SC water phase to settle and form a sediment bed over a two month period, while in the PC sample solids remained dispersed over the same time frame.
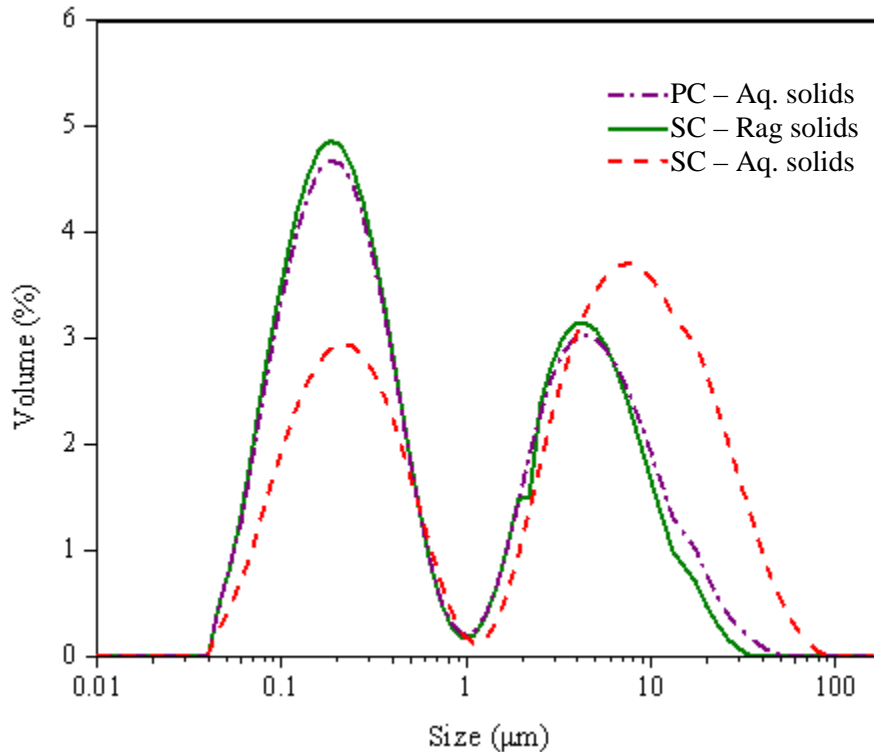
Figure 3-16: Particle size distribution of solids

With particle size distributions for PC-Aq.and SC-Rag approximately equivalent, it is not thought that particle size alone is responsible for the formation of a rag layer. Although size alone may not be the cause of formation of the rag layer, but a high fines and ultra-fines in the rag layer should be noted as a property of the solids collected from the rag layer.

3.9. THERMAL GRAVIMETRIC ANALYSIS (TGA)

Figure 3-17 illustrates TGA thermographs for a heat profile of 5 $^{\circ}$C/min. Details of measurements were explained in Sections 2.2.5 and 2.2.6.
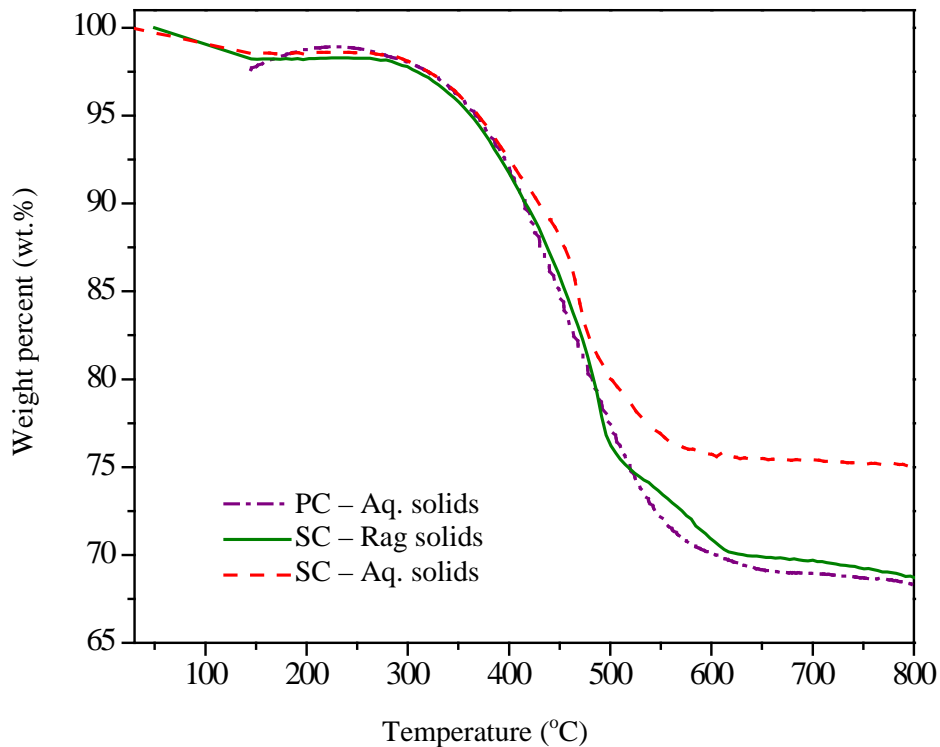
Figure 3-17: Comparison of Thermal gravimetric analysis of solid

TGA analysis shows that solids recovered from SC– Aq. solids exhibited a slightly lower mass loss compared with solids recovered from SC – Rag solids and PC– Aq. solids. This difference would mean that there is less organic matter on the surface of solids from SC-Aq. solids compared with SC – Rag solids and PC– Aq. solids. It was discussed in Section 3.8 that SC-Aq. solids are coarser than the rest of the solids. It is suspected that as a result of their larger size they may have less available surface area for organic matter

adsorption. This could explain the lower mass loss of SC-Aq. solids. However, the SC rag layer and PC water phase showed similar mass losses, which suggests that the amount of organic matter covering both solids is similar.

3.10. FTIR

Figures 3-18, 3-19 and 3-20 show expanded FTIR spectra across 1550-1750 cm^{-1}, 2700-3500 cm^{-1} and 3600-3720 cm^{-1} wavenumbers. All spectra are normalized at 1032cm^{-1} (highest intensity).

In Figure 3-18, the 2850 and 2925cm^{-1} bands are characteristic of the aliphatic hydrocarbons such as methyl and methylene groups. The intensities for PC– Aq. solids were slightly higher than SC-Rag solids. Hence, there is higher proportion of aliphatic hydrocarbons associated with the solids from PC– Aq. solids compared to SC – Rag solids. SC– Aq. Solids have the lowest amount of aliphatic hydrocarbons. The broadband present at 3000- 3500cm^{-1} corresponds to hydrogen bonding groups. This band has been reported as an indicator of functional groups with nitrogen in similar cases, (Gu et al. 2007; Wu et al. 2003). Unlike the aliphatic hydrocarbons band, the broadband at 3000-3500cm^{-1}, which is common in polar fraction of bitumen (Wu et al. 2003), has a higher intensity for SC-Rag solids than PC-Aq. solids. This indicates a different nature for the associated hydrocarbons of SC-Rag solids, which is further discussed in this section.

Figure 3-19 includes information relating to aromatic rings and C=O stretching. The band for aromatic rings (1600cm^{-1}) is higher for the SC rag layer solids compared to the other solids. This indicates that the insoluble organics present at the surface of the rag layer solids are more aromatic, hence asphaltenic. The broadband at 1680-1710cm^{-1} confirmed the presence of carboxylic acids. The presence of carboxylates is confirmed by the broadbands observed at 1560-1610cm^{-1} and 1310-1400 cm^{-1}.(Adegoroye et al. 2010) These bands have higher intensities for the rag layer solids. Sodium naphthenate is possibly the carboxylate found in the rag layer, (Czarnecki et al. 2007). These findings, like the ones from 3000-3500 cm^{-1}, also suggest a different nature in the type of organic matter adsorbed by SC-Rag solids

In Figure 3-20, the 3620cm^{-1} and 3698cm^{-1} doublet is characteristic of clays, (Gu et al. 2006; Wu et al. 2003). SC – Rag solids had the lowest intensity in this range, compared

to all other samples. This indicates that lower amounts of clays are present in the SC- Rag solids, compared to the other samples. This relates well with the earlier mineralogy findings.

It was understood from FTIR analysis that solids from SC– Aq. solids are covered by less organic matter which could be resulted by their coarser size, see Section 3.8. Thermal gravimetric analysis, Section 3.9, showed that equal amount of organic matter was adsorbed on PC-Aq. and SC-Rag solids. But the FTIR analysis revealed that solids from PC– Aq. solids were covered with hydrocarbons of a different nature from SC – Rag solids. The hydrocarbons covering solids from PC– Aq. solids were more aliphatic, while SC – Rag solids held more polar functional groups such as aromatics, carboxylic acids and functional groups with nitrogen. This difference in the types of associated organic matter could cause the SC-Rag solids to be more surface active and this difference in surface activity could be the reason why only one set of solids form the rag layer. The difference in mineralogy could have led to this difference in adsorbed organic matter which is discussed further in Section 3.12.
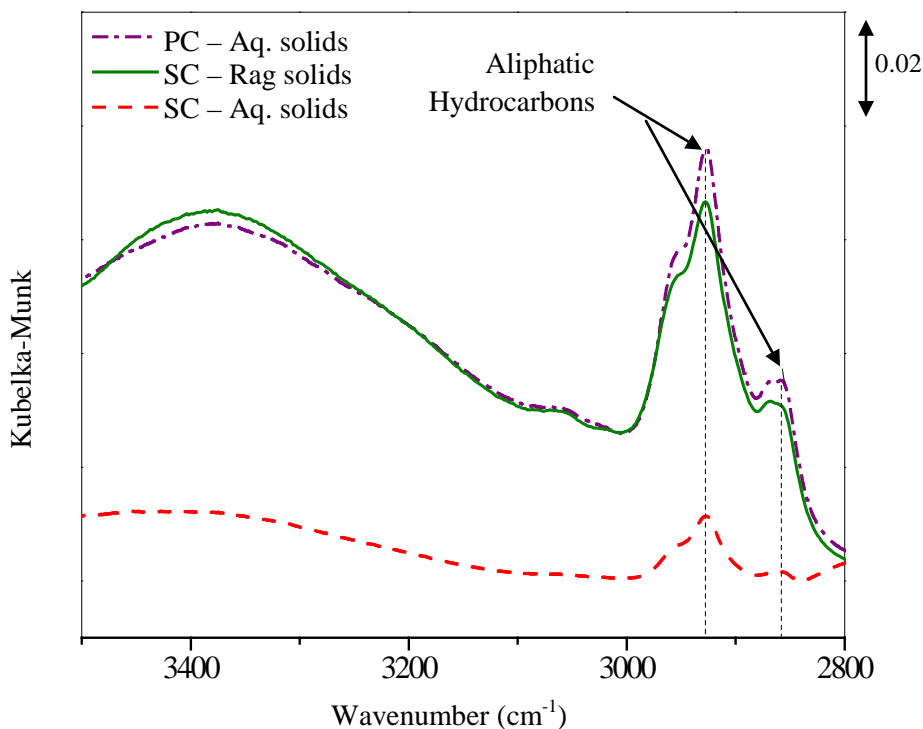
Figure 3-18: FTIR spectra at 2700-3500 cm^{-1} wavenumbers
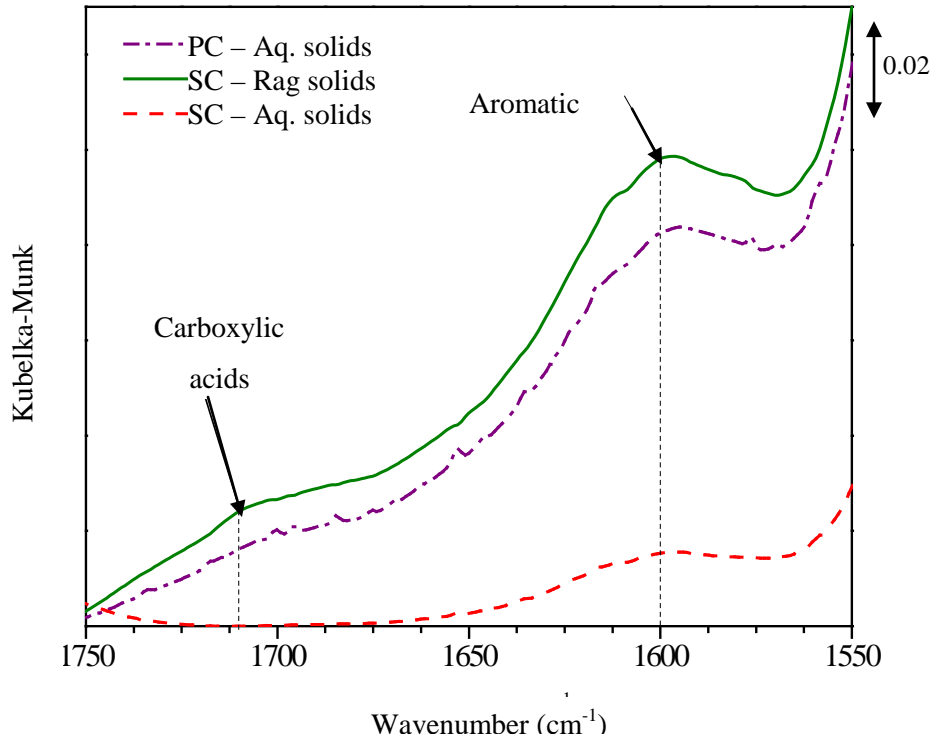
Figure 3-19: FTIR spectra 1550-1750 cm^{-1} wavenumbers
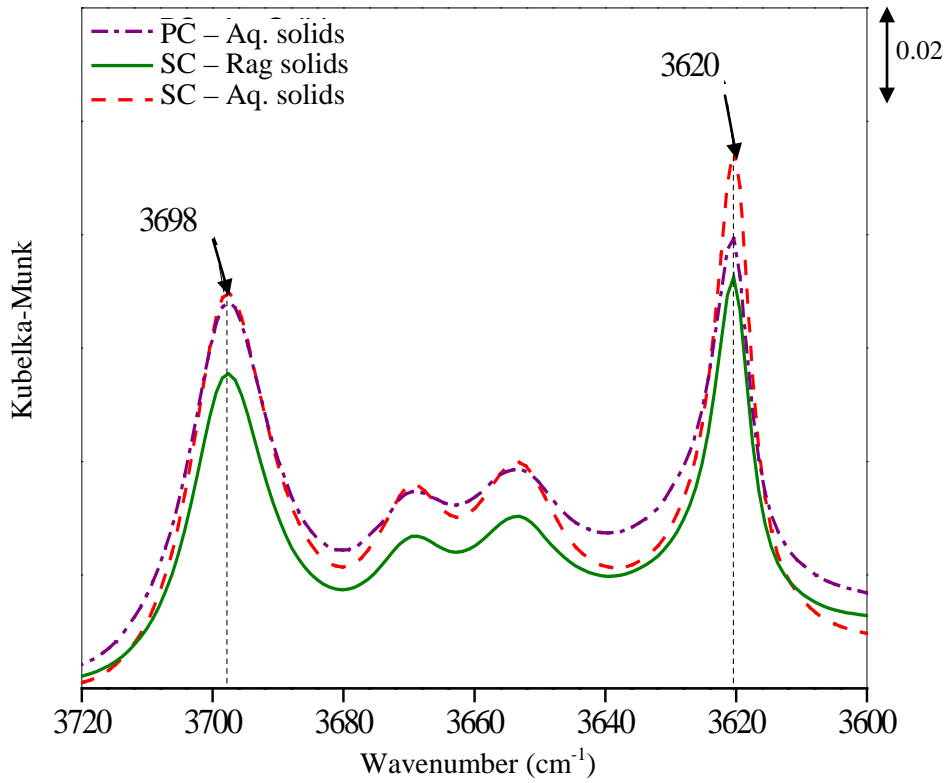
Figure 3-20: FTIR spectra at 3600-3720 cm^{-1} wavenumbers

3.11. WETTABILTY AND FILM FLOTATION

Solids wettability was determined using the film flotation technique, see discussion Section 2.2.7. Figure 3-21 shows the cumulative distribution curve of the film flotation experimental data for PC-Aq., SC-Rag and SC-Aq. solids. By examining this figure it is easily noted that SC-Aq. solids are more hydrophilic than PC-Aq. and SC-Rag solids as the distribution curve is excessively shifted to the right. Since PC-Aq. and SC-Rag solids curves are closely following each other, the critical wetting surface tension $\overline{\gamma}_c$ is calculated using the method explained in Section 2.2.7. This value allows semi-quantitative comparison of hydrophobicity between the solids used in this study. The frequency distribution curves are obtained from Figure 3-21 and displayed in Figure 3-22. The mean critical surface tension for PC-Aq. solids is 40.01mN/m and for SC-Rag solids is 36.62mN/m. Having a lower $\overline{\gamma}_c$, the SC-Rag solids are slightly more hydrophobic than PC Aq. solids.
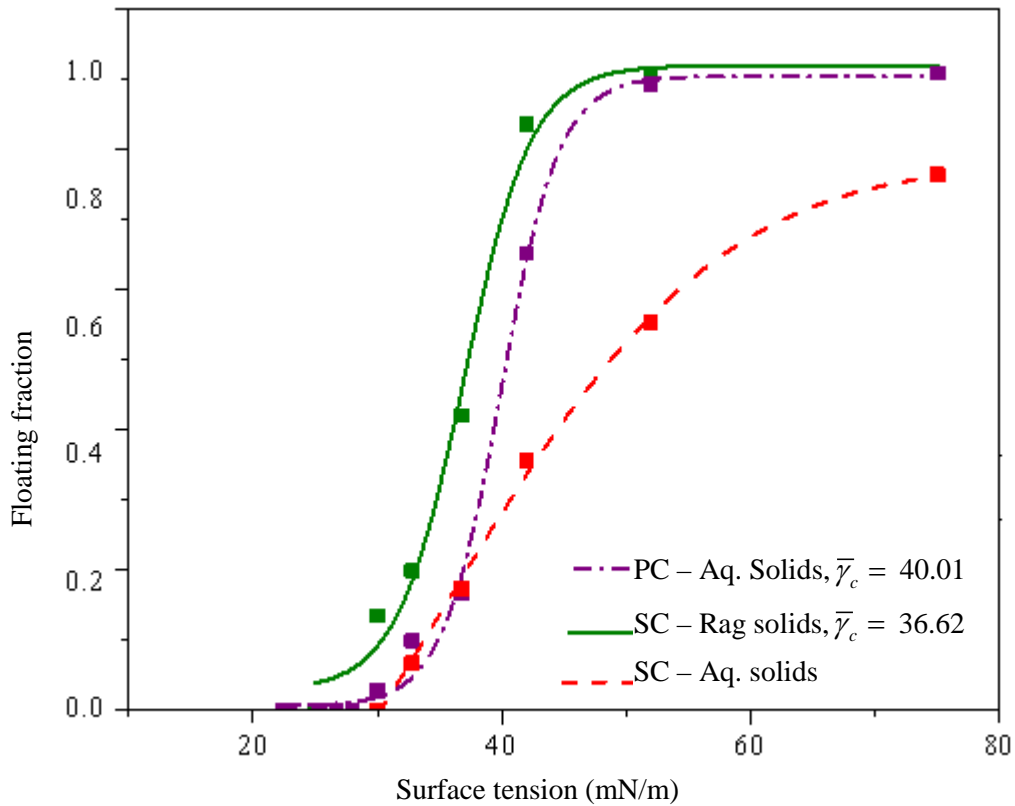
Figure 3-21: Cumulative distribution curve of solid particles

These results along with results obtained from FTIR analysis suggest that the organic matter attached to SC-Rag solids could be the reason of the observed increase in hydrophobicity. The higher amount of aromatics, nitrogen functional groups and carboxylics suggests a higher association of asphaltenes to SC-Rag solids. In other words, the more asphaltenic nature of the organic matter of SC-Rag solids has led to a higher hydrophobicity in addition to a higher polarity and surface activity. This property of SC-Rag solids could be related to their mineralogy, this is further discussed in Section 3.12.
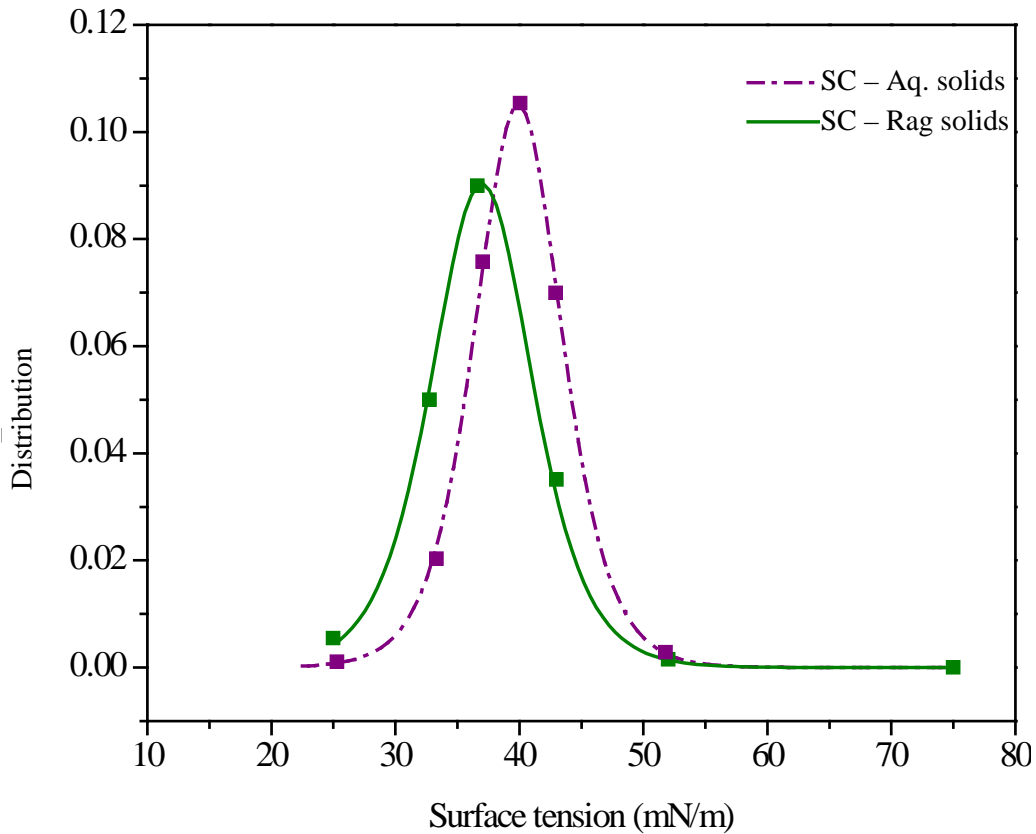
Figure 3-22: Distribution curve for solids

3.12. IRON, SIDERITE

XRD analysis showed that siderite, $FeCO_3$, and pyrite, FeS, which are iron minerals, are the major solids components in the rag layer. Therefore it is of interest to develop a greater understanding of their interfacial stabilizing capacity. After reviewing previous studies it is suggested that siderite associates with hydrocarbons and influences emulsion

stability in two manners: directly and also by transforming into iron ions and other iron compounds.

Mikula et al. (1989) found a correlation between the water content and siderite content of diluted bitumen produced from diluting froth with toluene. By running an X-ray analysis on toluene extracted solids from primary and secondary bitumen froth samples, it was found that a high siderite content, correspond to increasing water content in the final bitumen product. The authors concluded that iron-containing minerals such as siderite stabilize some of the water in oil emulsions formed during water-extraction processes of oil sands. Khademi (2012) also had a similar observation when comparing stability of water-in-toluene diluted bitumen emulsions stabilized by siderite, illite and kaolinite. The stability was determined by comparing coalescence probability of water droplets in the emulsion using the micropipette technique. She found that the emulsion stabilized by siderite is the most stable emulsion and had the lowest probability of coalescence.

It was observed in other studies that carboxylics can associate with carbonates, (Slade and Creek 1975; Vandegrift et al. 1980; Carter and Mitterer 1978; Chave 1965). Very strong association of oil shale organic matter with carbonate mineral through carboxylic acids has been reported by Vandegrift et al. (1980). In their study, the carboxylic acids were regarded as coupling agents between bitumen components, residual organic matter and the mineral matrix. Slade and Creek (1975) used carboxylic acids to float siderite from sand deposits containing kaolin clays to produce an iron-mineral-free sand to use in ceramic industry. In the current study solids with higher contents of siderite had a higher association with carboxylic acids, see Section 3.10.

Siderite is iron carbonate and like all other carbonates has ionic bond between its cation, Fe^{2+}, and anion CO_3^{2-}. This mineral is soft and soluble and is easily broken by weathering processes, (Stevenson 1982). Considering this, it may be possible that the presence of siderite in iron samples might lead to formation of iron oxides, iron hydroxides and also Fe^{3+}. Dixon and Weed (1989), Murad and Fischer (1988) and Chesworth (2008) explain that different forms of iron interact and convert to each other in soil. That is demonstrated in Figure 3-23. It is indicated that Fe (II) minerals (sulfides, carbonates, etc) oxidize to Fe (III) oxides which are very difficult to detect by XRD, (Kaminsky et al. 2009).

Mikula et al. (1989) compared the effect of iron compounds on stability of oil-in-water emulsions using two emulsions; one prepared with iron, added as $FeCl_3$ in water phase,

and a control emulsion without iron addition. Optical micrographs of the emulsions are shown in Figure 3-24. Image on the top shows the oil-in-water emulsion immediately after preparation and the middle image shows the control emulsion, prepared in the absence of iron, one minute after preparation. The top image represents both emulsions immediately after formation. The iron-free emulsion droplets begin to agglomerate one minute after formation. The bottom picture is the emulsion with iron and is easily spotted that one minute after formation, the emulsion is stable. It is concluded from this experiment that iron could contribute to emulsion stability.

Mikula et al. (1989) suggested that siderite, iron ions and iron hydroxides facilitate a bridge for organic constituents, mineral and water phase interactions. This bridge formation is related to the charge stabilizing caused by adsorption of polyvalent ions onto clays. In oil sands processing the clay particles are negatively charged, leading to repulsion between the clay particle and organic anions such as acidic functional groups of organic matter, COO^-. In order to overcome this repulsion, polyvalent cations, such as Ca^{2+}, Fe^{3+} and Al^{3+}, are required to form bridges between these components. Fe^{3+} forms strong bonds with organic matter with reactive groups such as: hydroxyl, carboxyl and phenoxyl, and strong chelating agents are required for displacing them, (Evans and Russel 1959; Greenland 1971; Alloway 1990).

Pools of Iron in Soils
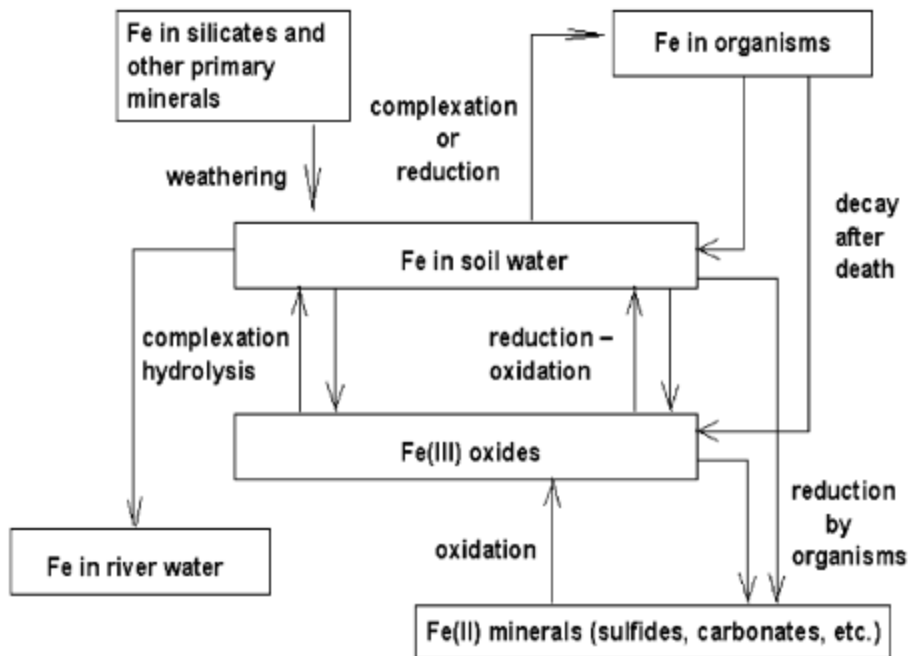
Figure 3-23: Illustration of how iron interacts in soil.

Oxides and hydrous oxides of iron could occur as surface coating on clays, (Eslahpazir et al. 2011). Kaminsky et al. (2009) observed an increase in contents of iron oxides in solids extracted from primary and secondary froth collected from a low-grade oil sand ore. Organic matter in the soil may be bound to oxides and hydrous oxides of iron by coordination (ligand exchange) and simple anion exchange.(Adegoroye et al. 2010; Stevenson 1982; Kotlyar et al. 1984; Greenland 1965; Kessick 1981; Adegoroye 2010)

The current project revealed that the major differences between rag forming solids and non-rag forming solids is in the abundance of siderite and a higher amount of polar compounds attached to them. Siderite has been considered as a major inorganic component in organic-mineral complexation, (Kotlyar et al. 1984). According to earlier studies, siderite associates well with carboxylic acids (Slade and Creek 1975; Vandegrift et al. 1980; Carter and Mitterer 1978; Chave 1965). The higher association of carboxylic acids and siderite agrees well with results from FTIR and XRD analysis which indicate a higher association of carboxylic acids and asphaltenes with rag forming solids, sections

3.7 and 3.10. The surface coatings of the solids make them more hydrophobic and surface active, Section 3.11 and this enables them to stabilize emulsions.
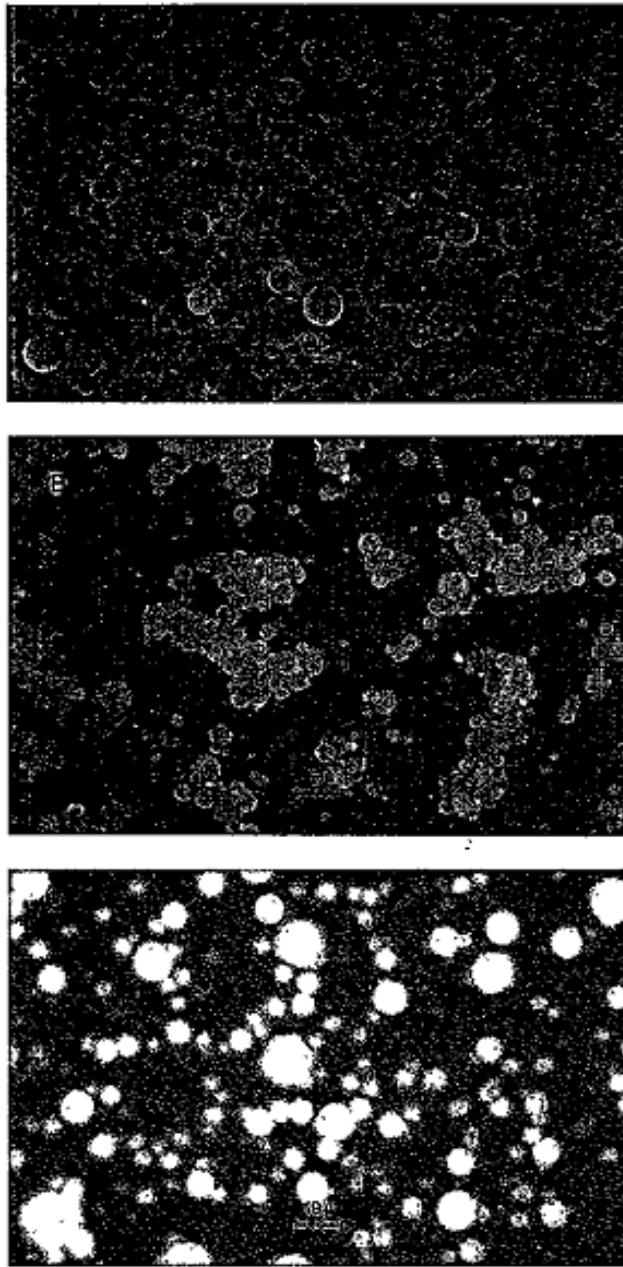
Figure 3-24: Image on top: oil in water emulsion immediately after preparation. Image in middle: emulsion without iron. Image at bottom: emulsion with iron.

Moreover it is possible that siderite, pyrite and perhaps other possible forms of present iron form bridges between water droplets, other minerals and bitumen components. This could have lead to formation of networks and structures in the rag layer. However, more studies are necessary in order to completely understand the emulsion stabilizing mechanism of iron-compounds and their ability in formation of bridges between emulsion constituents.

4. SUMMARY AND CONCLUSION

A viscous layer forms at the planar interface of water and diluted bitumen during removal of water from water-in-oil emulsions. This unwanted viscous layer which is known as the rag layer disturbs removal of water droplets from diluted bitumen. The oil phase trapped within the rag layer is not recoverable and hence formation of the rag layer reduces diluted bitumen recovery.

In this study samples from overflow of primary (PC) and secondary hydrocyclones (SC) of a naphthenic froth treatment plant are characterized and compared. The rag layer can only be regenerated from samples obtained from the overflow of the secondary hydrocyclones. The reproduction of the rag layer is achieved by shaking the jars containing samples from the overflow of the secondary hydrocyclones and providing them with sufficient time to settle in 100 mL cylinders. The thickness and viscosity of the rag layer increase over a period of 14 days in the cylinders. By transferring the material from a jar (wide container) to a cylinder (narrow container) the stability of the rag layer improves, meaning that it does not break, settle down or disappear over a year and it is very viscous and does not flow.

The rag layer is a complex emulsion with a continuous oil phase which does not diffuse in n-heptane, but it diffuses very well in toluene. Upon diffusion in toluene, many small and scattered water droplets are revealed in the rag layer.

The density of the rag layer is an intermediate value between the bottom water phase and the top solids-free oil layer. The density of the rag layer increases by 2% as the rag layer approaches the interface of the water phase. The water content of the rag layer also increases throughout the rag layer from 22 wt% to 28 wt% at the water interface. This increase in the water content of the rag layer corresponds to the increase in the density of the rag layer. The solids content of the rag is relatively constant at 14 wt% throughout the rag layer.

SC – Rag solids are compared with PC - Aq. solids and SC – Aq. solids. This comparison revealed the following facts:

- *Particle size distribution:* The particle size distribution of SC – Rag solids is quite similar to that of the PC - Aq. solids. Most of the solids are smaller than 2

μm. SC – Aq. solids are slightly larger. The minor differences in the particle size distribution are not found as a major contributing factor to rag formation.

- *Mineralogy:* SC – Rag solids have a different mineralogy from PC - Aq. solids and SC – Aq. solids. Heavy minerals, most specifically siderite, are more abundant in SC – Rag solids than the other solid samples. Alternatively, SC – Aq. solids and PC - Aq. solids hold higher amount of clays compared to the rag layer. This difference in mineralogy could be a key contributing factor in rag formation.

- *Associated organic matter:* The amount of organic material adsorbed on SC – Aq. solids is less than that for PC - Aq. solids and SC – Rag solids. This could correspond to their coarser size. Amount of organic matter adsorbed on PC - Aq. solids and the rag layer is similar. FTIR analysis of the solids showed that the organic matter adsorbed on surface of PC - Aq. solids is different from SC – Rag solids. Organic matter of PC - Aq. solids hold more aliphatic hydrocarbons compared to that for the rag layer solids. Meanwhile, organic matter on surface of solids from the rag layer holds a higher content of polar functional groups such as carboxylic acids and aromatics-asphaltenes. This could be related to the ability of iron minerals in adsorbing more polar groups.

- *Hydrophobicity:* The increased hydrophobicity in SC – Rag solids could be linked to the different type of organic matter adsorbed on the surface of the solids. This difference may have been caused by the difference in the adsorbed organic matter ruled by their mineralogy. In other words, it is possible that the heavy minerals, most specifically siderite, had a higher affinity for polar hydrocarbon groups, such as carboxylics, than clays.

By putting together all the findings from this work and earlier studies the rag layer is more understood:

Saadatmand and Yarranton (2008) suggest that the slow coalescene rate of water droplets with each other and the planar water phase contribute to formation of the rag layer. Outer surface of water droplets is covered with irreversibly absorbed asphaltenes (Freer and Radke 2004) and solid particles (Binks and Lumsdon 2000b). Upon coalescence of two droplets their outer surface becomes more stable as the degree of coverage of the surface by the surface active materials increases. These changes in the interfacial film of water droplets reduce the droplets coalescence speed and eventually prevent the droplets from

coalescing with the continuous water phase, (Arditty et al. 2003). As the droplets ability to coalescence with the planar interface is reduced they could stack on top of each other. A similar event could have occurred in this study and evidence of such event is spotted in the increase in the water content close to the interface.

The fines and ultra-fines solids are present at the interface of water droplets, contributing to emulsion stability. They could also be dispersed in the oil phase in forms of flocs settling as a result of their gravity. These flocs which were found to be mostly siderite are associated with carboxylics and aromatics and could interact with emulsified water droplets since the interface of water droplet is covered by material of the same nature. Hence, networks of flocculates similar to those observed in Section 3.4 will form within the water-in-oil emulsion. By forming networks the viscosity of the oil phase of the water in-oil-emulsion increases. This highly viscous emulsion which holds solid-water-oil networks within is called the rag layer.

In conclusion, the experimental studies conducted in our study suggest that the polar organic matter such as asphaltenes contribute to formation of the rag layer. At presence of heavy minerals such as siderite and pyrite, the association of the polar organic matter increases. The attachment of the organic matter is higher for fines and ultra-fines compared to coarser solids. It is recommended for future studies to compare the ability of clays, such as kaolinite and illite, with siderite in stabilizing emulsions.

BIBLIOGRAPHY

1. Adegoroye, A. (2010). Characterization of solids isolated from different oil sands ores. University of Alberta, Edmonton.

2. Adegoroye, A., Wang, L., Omotoso, O., Xu, Z., and Masliyah, J. H. (2010). "Characterization of organic-coated solids isolated from different oil sands." *The Canadian Journal of Chemical Engineering,* 88(2), 462-470.

3. Ali, M. F., and Alqam, M. H. (2000). "The role of asphaltenes, resins and other solids in the stabilization of water." *Fuel,* 79(11), 1309-1316.

4. Alloway, B. J. (1990). *Heavy metals in soil.* John Wiley & Sons, Inc.

5. Angle, C. W., Dabros, T., and Hamza, H. A. (2007). "Demulsifier effectiveness in treating heavy oil emulsion in the presence of fine sands in the production fluids." *Energy Fuels,* 21(2), 912-919.

6. Arditty, S. S., Whitby, C. P., Binks, B. P., Schmitt, V. V., & Leal-Calderon, F. F. (2003). "Some general features of limited coalescence in solid-stabilized emulsions." *European Physical Journal E -- Soft Matter*, 11(3), 273-281.

7. Aveyard, R., Binks, B., and Clint, J. (2003). "Emulsions stabilised solely by colloidal particles." *Advances in Colloid and Interface Science,* 100, 503-546.

8. Bensebaa, F., Kotlyar, L. S., and Sparks, B. D. (2000). "Organic coated solids in Athabasca bitumen: Characterization and process implications." *The Canadian Journal of Chemical Engineering,* 78(4), 610–616.

9. Binks, B. P., and Kirkland, M. (2002). "Interfacial structure of solid-stabilised emulsions studied by scanning electron microscopy." *Physical Chemistry Chemical Physics,* (15), 3727-3733.

10. Binks, B. P., and Lumsdon, S. O. (2000a). "Catastrophic phase inversion of water-in-oil emulsions stabilized by hydrophobic silica." *Langmuir,* 16(6), 2539–2547.

11. Binks, B. P., and Lumsdon, S. O. (2000b). "Influence of particle wettability on the type and stability of surfactant-free emulsions." *Langmuir,* 16(23), 8622-8631.

12. Carter, P. W., and Mitterer, R. M. (1978). "Amino-acid composition of organic-matter associated with carbonate and non-carbonate Sediments." *Geochimica et Cosmochimica Acta,* 42(8), 1231-1238.

13. Chave, K. E. (1965). "Carbonates - association with organic matter in surface seawater." *Science,* 148(3678), 1723-1724.

14. Chesworth, W. (2008). "Iron oxides." *Encyclopedia of soil science,* 363-369.

15. Czarnecki, J., Moram, K., and Yang, X. (2007). "On the "rag layer" and diluted bitumen froth dewatering." *The Canadian Journal of Chemical Engineering,* 85 748-755.

16. Dixon, J. B., and Weed S. B. (1989). Minerals in soil environments. Soil Science Society of America.

17. Eslahpazir, R., Kupsta, M., Liu, Q., and Ivey, D. G. (2011). "Sample preparation method for characterization of fine solids in Athabasca oil sands by electron microscopy." *Energy Fuels,* 25(11), 5158-5164.

18. Evans, L. T., and Russel, E. W. (1959). "The adsorption of humic and fulvic acid by clays." *Journal of Soil Science,* 10(1), 119-132.

19. Feng, X., Xu, Z., and Masliyah, J. H. (2009). "Biodegradable polymer for demulsification of water-in-bitumen emulsions." *Energy Fuels,* 23(1), 451-456.

20. Freer, E. M., and Radke, C. J. (2004). "Relaxation of asphaltenes at the toluene/water interface: Diffusion exchange and surface rearrangement." *Journal of Adhesion,* 80(6), 481-496.

21. Frising, T., Noɪ̈k, C., and Dalmazzone, C. (2006). "The liquid /liquid sedimentation process: From droplet coalescence to technologically enhanced water /oil emulsion gravity separators: A review." *Journal of Dispersion Science and Technology,* 27(7), 1035-1057.

22. Fuerstenau, D., Ciao, J., and Williams, M. (1991). "Characterization of the wettability of solid particles by film flotation 1. Experimental investigation." *Colloids and Surfaces,* 60 127-144.

23. Greenland, D. J. (1965). Soil and fertilizers, 415-500.

24. Greenland, D. J. (1971). "Interactions between humic and fulvic acids and clays." *Soil Science,* 111(1), 34-41.

25. Gu, G., Xu, Z., Nandakumar, K., and Masliyah, J. H. (2002). "Influence of water-soluble and water-insoluble natural surface active components on the stability of water-in-toluene-diluted bitumen emulsion." *Fuel,* 81(14), 1859-1869.

26. Gu, G., Zhang, L., Wu, X. A., Xu, Z., and Masliyah, J. (2006). "Isolation and characterization of interfacial materials in bitumen emulsions." *Energy Fuels,* 20, 673-681.

27. Gu, G., Zhang, L., Xu, Z., and Masliyah, J. (2007). "Novel bitumen froth cleaning device and rag layer characterization." *Energy Fuels,* 21(6), 3462–3468.

28. Jiang, T., Hirasaki, G. J., Miller, C. A., and Moran, K. (2008). "Using silicate and pH control for removal of the rag layer containing clay solids formed during demulsification." *Energy Fuels,* 22(6), 4158–4164.

29. Jiang, T., Hirasaki, G. J., Miller, C. A., and Ng, S. (2011). "Effects of clay wettability and process variables on separation of diluted bitumen emulsion." *Energy Fuels,* 25(2), 545-554.

30. Jiang, T., Hirasaki, G., and Mill, C. (2007). "Diluted bitumen water-in-oil emulsion stability and characterization by nuclear magnetic resonance (NMR) measurements." *Energy Fuels,* 21(3), 1325–1336.

31. Kaminsky, H. A. W., Etsell, T. H., Ivey, D. G., and Omotso, O. (2009). "Distribution of clay minerals in the process streams produced by the extraction of bitumen from Athabasca oil sands." *The Canadian Journal of Chemical Engineering* 87(1), 85-93.

32. Kessick, M. A. (1981). Surface phenomena in enhanced oil recovery. 559.

33. Khademi, S. (2012). *Effect of Solid Contamination on Stability of Model Oil-Water Emulsions, Master of Science Thesis.* University of Alberta, Edmonton.

34. Kilpatrick, P., McLean, D., and Peter K. (1997). "Effects of asphaltene solvency on stability of water-in-crude-oil emulsions." *Journal of Colloid and Interface Science,* 189, 242-253.

35. Kilpatrick, P., and Spiecker, M. (2001). "Asphaltene emulsions." *Encyclopedic Handbook of Emulsion Technology,* CRC Press, 707-730.

36. Kotlyar, L. S., Sparks, B. D., and Kodama, H. (1984). "Some chemical and mineralogical properties of fine solids derived from oil sands." *AOSTRA Journal of Research,* 1(2), 99-106.

37. Kotlyar, L. S., Sparks, B. D., and Woods, J. R. (1998). "Distribution and types of solids associated with bitumen." *Petroleum Science and Technology,* 16(1-2), 1-19.

38. Kotlyar, L. S., Sparks, B. D., Woods, J. R., and Chung, K. H. (1999). "Solids associated with the asphaltene fraction of oil sands bitumen." *Energy Fuels,* 13(2), 346-350.

39. Liu, J., Xu, Z., and Masliyah, J. H. (2004). "Role of fine clays in bitumen extraction from oil sands." *AIChE Journal, 50*(8), 1917-1927.

40. Liu, J., Xu, Z., and Masliyah, J. H. (2005). "Processability of oil sand ores in Alberta." *Energy Fuels,* 19(5), 2056-2063.

41. Masliyah, J. H. (2009). *Fundamentals of oil sands extraction- ChE 534 course notes.* University of Alberta, Edmonton.

42. Masliyah, J. H., Zhou, Z. J., Xu, Z., Czarnecki, J., and Hamza, H. (2008). "Understanding water-based bitumen extraction from Athabasca oil sands." *The Canadian Journal of Chemical Engineering, 82*(4), 628-654.

43. McLean, J.D., and Kilpatrick, P. (1997). "Effects of asphaltene aggregation in model heptane-toluene mixtures on stability of water-in-oil emulsions." *Journal of Colloid Interface Science,* 196 23-34.

44. Mikula, R. J., Munoz, V. A., and Lam, W. W. (1989). "Correlations between oil sands minerals and processing characteristics." *Journal of Canadian Petroleum Technology,* 28(6), 29-32.

45. Mohamed, R. S., Ramos, A. C. S., and Loh, W. (1999). "Aggregation behavior of two asphaltenic fractions in aromatic solvents." *Energy Fuels,* 13(2), 323-327.

46. Mullins, O. and Sheu, E. Y. (1998). Structures and dynamics of asphaltenes. Springer, New York.

47. Murad, E., and Fischer, W. R. (1988). "Geobiochemical cycle of iron." *Iron in Soils and Clay Minerals,*1-18 .

48. Ohsol, E. O. (1999). "Process for recovering high quality oil from refinery waste emulsions." (US Patent 5882506).

49. Rosales, S., Machin, I., Sanchez, M., Rivas, G., and Ruette, F. (2006). "Theoretical modeling of molecular interactions of iron with asphaltenes from heavy crude oil." *Journal of Molecular Catalysis A-Chemical,* 246(1-2), 146-153.

50. Saadatmand, M., and Yarranton, H. W. (2008). "Rag layers in oil sand froths." *Industrial & Engineering Chemistry Research,* 47(22), 8828–8839.

51. Samiei, S. (2007). "Role of ultra-fine solid fractions on rheology of oil sands suspensions." PhD thesis, University of Alberta, Canada.

52. Sjoblom, J., Askea, N., Auflema, I. H., Brandala Ø., Havrea, T. E., Sæthera, Ø., Westvikb, A., Johnsenb, E. E., and Kallevikb, H. (2003). "Our current understanding of water-in-crude oil emulsions.: Recent characterization techniques and high pressure performance." *Advances in Colloid and Interface Science,* 100-102 399-473.

53. Sjoblom, J., Ese, M., Lu, W., and Yang, X. (2001a). "Film properties of asphaltenes and resins." *Encyclopedic handbook of emulsion technology,* CRC Press, 525-540.

54. Slade, W. W., and Creek, W. (1975). "Benefication of siderite contaminated sand." (US Patent 3914387).

55. Stevenson, F. J. (1982). Humus chemistry—genesis, composition, reactions, John Wiley and Sons, Inc, New York, 374-400.

56. Strausz O. P., Mojelsky, T. W., and Lown E. M. (1992). "The molecular structure of asphaltene: an unfolding story." *Fuel,* 71(12), 1355–1363.

57. Sztukowski, D. M., and Yarranton, H. W. (2005). "Oilfield solids and water-in-oil emulsion stability." *Journal of Colloid and Interface Science,* 285(2), 821-833.

58. Tambe, D. E., and Sharma, M. M. (1993). "Factors controlling the stability of colloid-stabilized emulsions: I. An experimental investigation." *Journal of Colloid and Interface Science,* 157(1), 244-253.

59. Tan, K. H. (2009). Environmental soil science, Marcel Dekker, New York, 75-77.

60. Trong, D., Jha, R., Wu, S., Tannant, D., Masliyah, J. H., and Xu, Z. (2009). "Wettability determination of solids isolated from oil sands." *Colloids and Surfaces A: Physicochemical and Engineering Aspects,* 337(1-3), 80-90.

61. Urdahl, O., Movik, A. E., and Sjoblom, J. (1993). "Water-in-crude oil-emulsions from the Norwegian continental-shelf .8. surfactant and macromolecular destabilization." *Colloids and Surfaces A-Physicochemical and Engineering Aspects,* 74(2-3), 293-302.

62. Vandegrift, G. F., Winans, R. E., Scott, R. G., and Horwitz, E. P. (1980). "Quantitative study of the carboxylic acids in Green river oil shale bitumen." *Fuel,* 59 627-633.

63. Varadaraj, R., and Brons, C. (2007). "Molecular origins of crude oil interfacial activity Part 3: Characterization of the complex fluid rag layer formed at crude." *Energy Fuels,* 21 1617-1621.

64. Wang, S. (2011). " Understanding stability of water-in-diluted bitumen emulsions by colloidal force measurements, PhD. Dissertation " PhD thesis .

65. Whitesides, T. H., Ross, D. S. (1995) "Experimental and theoretical-analysis of the limited coalescence process - stepwise limited Coalescence" *Journal of Colloid and Interface Science*, 169(1), 48-59

66. Wu, X. (2003). "Investigating the stability mechanism of water-in-diluted bitumen emulsions through isolation and characterization of the stabilizing materials at the interface." *Energy Fuels,* 17(1), 179-190.

67. Yan, N., Gray, M. R., and Masliyah, J. H. (2001). "On water-in-oil emulsions stabilized by fine solids." *Colloids and Surfaces A: Physicochemical and Engineering Aspects,* 193(1-3), 97-107.

68. Yan, Z., Elliott, J., and Masliyah, J. (1999). "Roles of various bitumen components in the stability of water-in-diluted-bitumen emulsions." *Journal of Colloid and Interface Science,* 220(2), 329–337.

69. Yang, F. (2010). *Impact of solvents treatment on the wettability of froth solids, Master of Science Thesis.* University of Alberta, Edmonton.

70. Yang, X., and Czarnecki, J. (2002). "The effect of naphtha to bitumen ratio on properties of water in diluted bitumen emulsions." *Colloids and Surfaces A-Physicochemical and Engineering Aspects,* 211(2-3), 213-222.

71. Yang, X., Hamza, H., and Czarnecki, J. (2004). "Investigation of subfractions of athabasca asphaltenes and their role in emulsion stability." *Energy Fuels,* 18(3), 770-777.

72. Yen, T. F., Boucher, L. J., Dickie, J. P., Tynan, E. C., and Vauchan, G. B. (1969). "Vanadium complexes and porphyrins in asphaltenes." *Journal of the Institute of Petroleum,* 55(542), 87-99.

73. Yeung, A., Dabros, T., Masliyah, J., and Czarnecki, J. (2000). "Micropipette: a new technique in emulsion research." *Colloids and Surfaces A-Physicochemical and Engineering Aspects,* 174(1-2), 169-181.

74. Yong, R. N., and Sethi, A. J. (1978). "Mineral particle interaction control of tar sand sludge stability." *Journal of Canadian Petroleum Technology,* 17(4), 76-83.

75. Zhang, L., Xu, Z., and Mashyah, J. (2003). "Langmuir and Langmuir-Blodgett films of mixed asphaltene and a demulsifier." *Langmuir,* 19(23), 9730-9741.

76. Zhou, Z. A., Xu, Z., Masliyah, J. H., and Czarnecki, J. (1999). "Coagulation of bitumen with fine silica in model systems." *Colloids and Surfaces A: Physicochemical and Engineering Aspects,* 148(3), 199-211.

APPENDIX

Diffraction patterns of the three solid samples mentioned in Section 3.7.
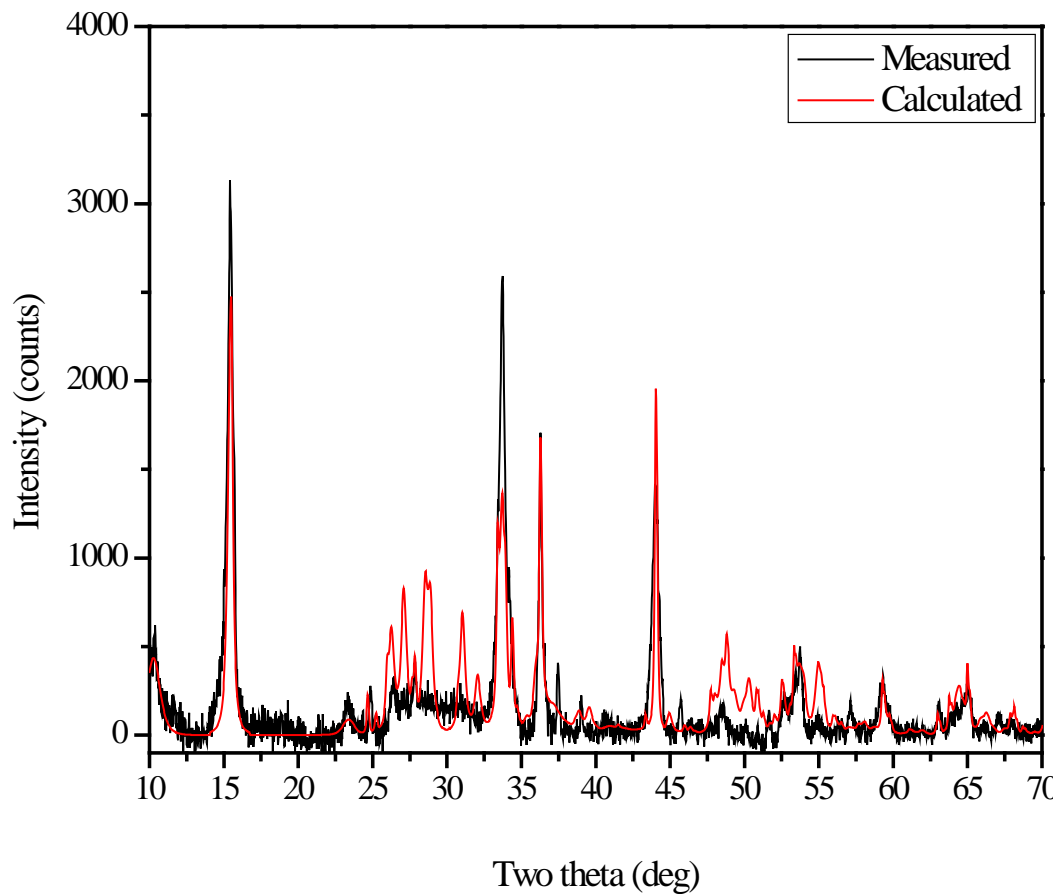
Figure A-1: X-ray diffraction pattern for solids from water phase of PC
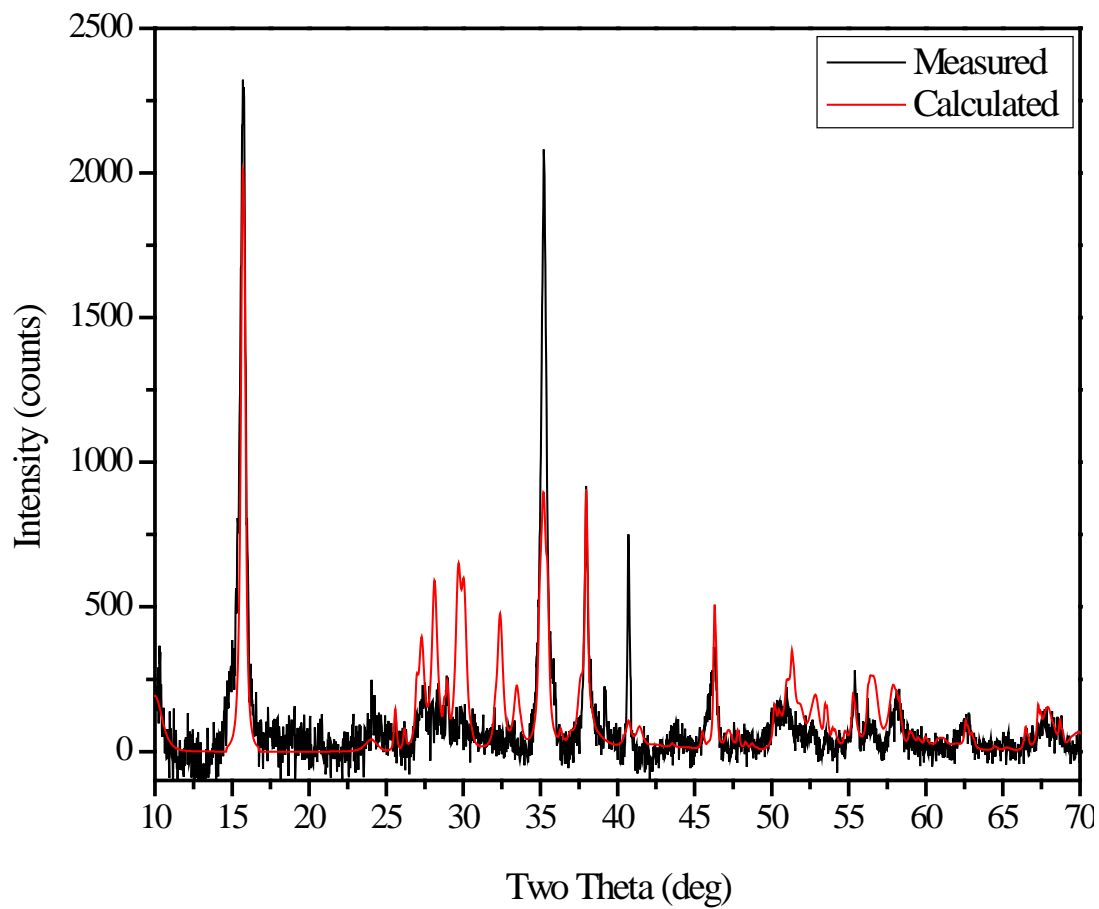
Figure A-2: X-ray diffraction pattern for solids from water phase of SC
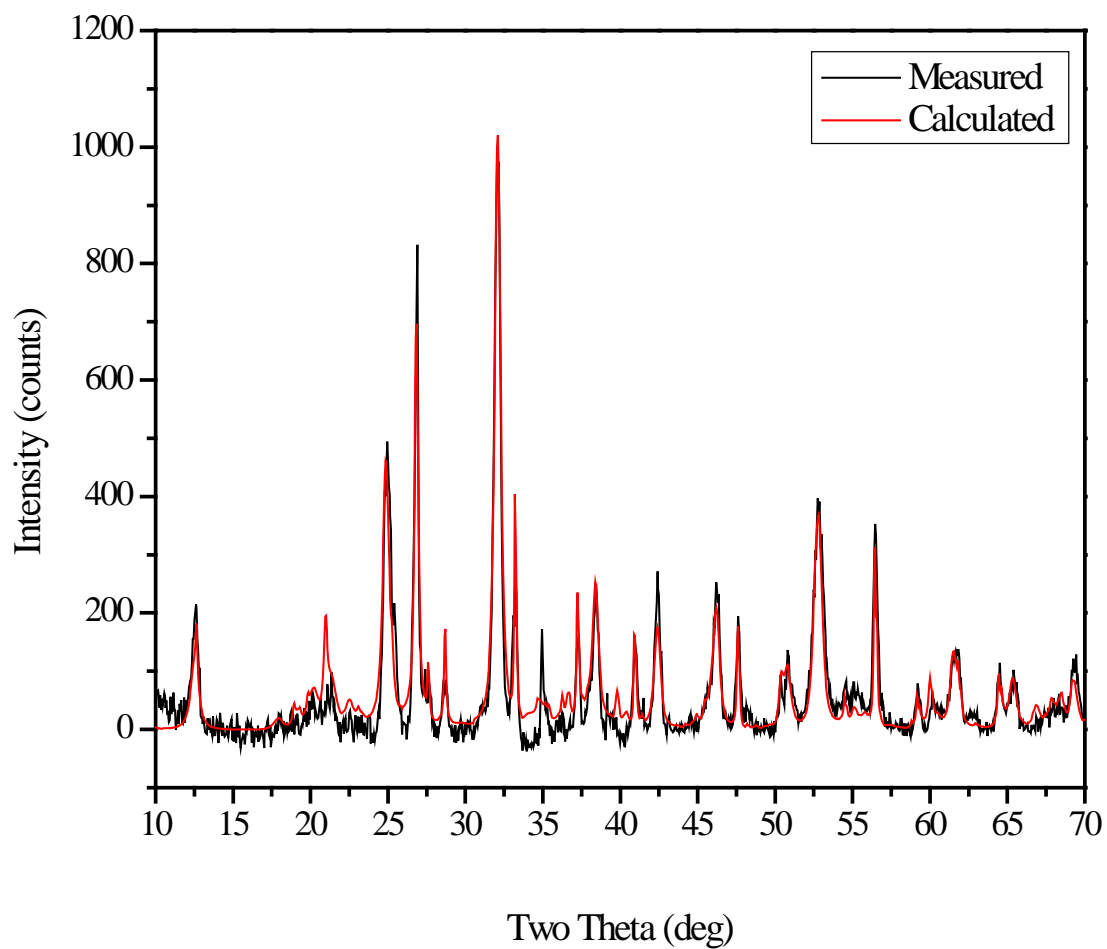
Figure A-3: X-ray diffraction pattern for solids from the rag layer of SC